1,2-Palladasilacyclobutene: The Missing Link in the Pd-Catalyzed Annulation of Alkynes for the Silirene-to-Silole Transformation

Marc Devillard, Chiara Dinoi, Iker Del rosal, Clément Orione, Marie Cordier, Gilles Alcaraz

Inorganic Chemistry

pubs.acs.org/IC Article

1,2-Palladasilacyclobutene: The Missing Link in the Pd-Catalyzed Annulation of Alkynes for the Silirene-to-Silole Transformation

Marc Devillard,* Chiara Dinoi, Iker Del Rosal, Clément Orione, Marie Cordier, and Gilles Alcaraz*

Cite This: https://doi.org/10.1021/acs.inorgchem.3c00045 Read Online

ACCESS | Metrics & More | Article Recommendations | Supporting Information

ABSTRACT: The palladium-catalyzed annulation reaction of alkynes enables an attractive approach to siloles. Their access from silirenes and terminal alkynes proved rather general, involving reactive intermediates that have remained elusive to date. Starting from 1,2-bis(3-thienyl)silirene as a source of photochromic siloles, the mechanism of the annulation reaction has been revisited, and palladasilacyclobutenes resulting from the activation of the silirene could be isolated and thoroughly characterized (NMR, X-ray, and DFT). Their role as reactive intermediates and their fate in the course of the reaction were also studied in situ. In combination with in-depth DFT calculations, a clearer picture of the mechanism and the reactive key species is disclosed.

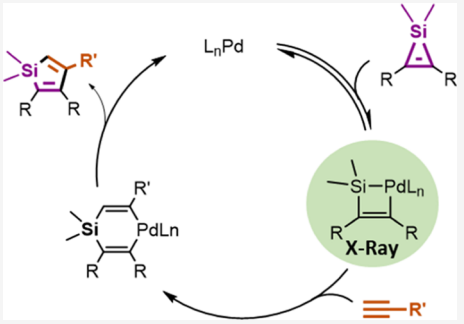

INTRODUCTION

The chemical behavior of three-membered ring heterocycles is mostly dictated by the release of the ring strain[1] as the main driving force, with a strong influence both of the nature of the embedded heteroelement and of the degree of unsaturation of the cycle.[2] They have proven to be molecules of choice in organic synthesis, offering a wide range of reactivity and a versatile chemistry, especially when combined with catalysis.[3] In particular, they enable the synthesis of higher heterocyclic structures either via intramolecular ring expansion or through insertion reactions in the presence of an unsaturated partner. This approach provides an attractive methodology for the installation of the heteroelement, particularly in the course of new π-conjugated molecules incorporating heavier p-block elements.[4] In this context, the chemistry of silacycles (silicon rings with 3,[5] 4,[6] 5,[6d,7] or more[8] members) is probably the more mature research field driven by that of silacyclopentadienes (siloles) and their peculiar electronic properties.[9] Over the years, this interest has turned siloles into important synthetic targets and has motivated significant efforts toward methodological development.[10] While preparation of siloles relied generally on uncatalyzed transformations involving stoichiometric amounts of organometallic reagents, most recent achievements are based on catalytic routes, mainly using rhodium or palladium complexes.[11] They proceed either (i) intramolecularly from acyclic silanes through arylations of Si−X (X = CH_3, H) bonds[12] and C−C bond formation between peripheral substituents[13] or (ii) intermolecularly by reaction of an alkyne with a suitable silicon-based reagent.[14] Within this second category, the use of silacyclopropene (silirene) as a direct precursor of siloles is a very attractive strategy, as it takes advantage of both the inherent reactivity of the silicon-containing precursor and the possibilities offered by the large pool of alkynes. This Pd-catalyzed annulation of an alkyne in the presence of a silirene was reported in the substance as early as 1977 by Seyferth in his seminal studies.[15] Despite more recent efforts to improve the methodology,[16] this promising reaction has remained globally underutilized with respect to its potential in organic synthesis. In this setting, we have recently described an efficient methodological approach to photochromic siloles[17] with a dithienylethene (DTE) skeleton. The strategy relies on the Pd-catalyzed [3 + 2]-annulation reaction of alkynes with a 1,2-bis(3-thienyl)silirene **1** (Scheme 1).

This divergent methodology proved rather general, tolerant to a variety of functional groups, and could even be extended to the post-polymerization functionalization of PPMA-type

Scheme 1. Palladium-Catalyzed Synthesis of Photochromic Siloles by Annulation Reaction of Alkynes with a Silacyclopropene

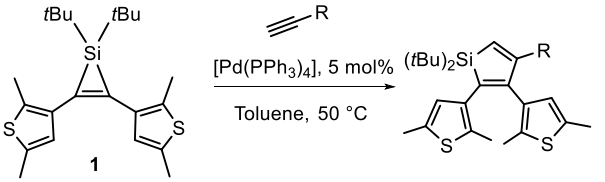

Received: January 5, 2023

(polypropar-gylmethacrylamide) polymers displaying terminal alkyne functionalities.[17] While this transformation can be formally seen as the regiospecific insertion of the C≡C triple bond of a terminal alkyne into one of the two endocyclic Si−C single bonds of silirene, some aspects of this chemical transformation remain unclear when compared with the mapping of the general reactivity of silirenes with alkynes under palladium catalysis and the different scenarios related to the interplay of the silirene/alkyne pair with the metal (Scheme 2).

Scheme 2. Different Scenarios of the Palladium-Catalyzed Reaction of Silirenes with Alkynes (for Route (1) See Refs 15d 21a 21b,; for Route (2) See Refs 15a 15b 15d 16a 16b,; for Route (3) See Ref 16b; for Route (4) See Ref 21b; and for Route (5) See Ref 18)

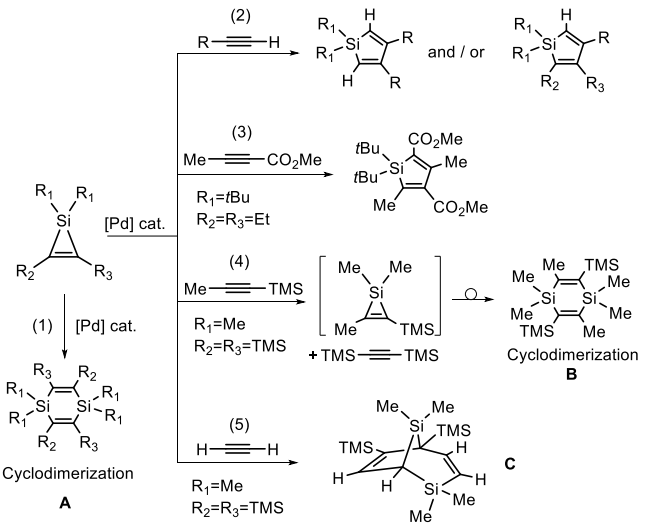

Initially, the mechanism of the formation of siloles (Scheme 2—route (2) and (3)) was envisaged to proceed through the intermediacy of a putative 1,2-palladasilacyclobutene **I**, resulting from the oxidative addition (OA) of Pd(0) to the silirene (Scheme 3).[18]

Later, this catalytic reaction was extended successfully by the group of Woerpel to 1,1-di-*tert*-butyl-silirenes, affording selective 3-phenylsiloles.[16a,c] On this basis, they proposed a more complete picture of the catalytic cycle involving the

Scheme 3. Commonly Accepted Catalytic Cycle for the Palladium-Catalyzed Annulation Reaction of Alkynes with a Silirene

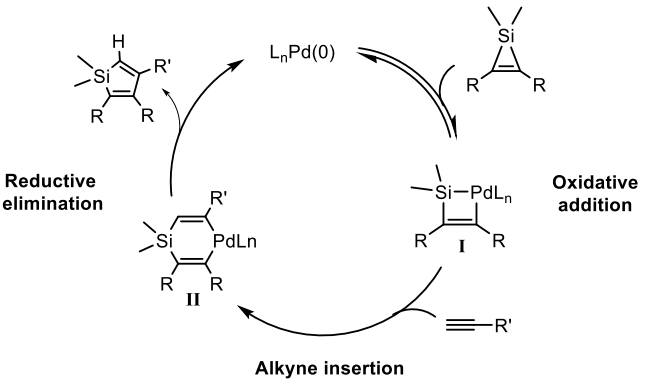

insertion of the alkyne partner into the Pd−Si bond of the metallacycle **I** to form a 1,4-palladasilacyclohexadiene **II**, followed by a classical reductive elimination step with the release of the silole product (Scheme 3). This commonly accepted mechanism remains, however, partly hypothetical due to the lack of compelling evidence, particularly in the form of isolated organometallic intermediates and their subsequent reactivity. On this basis, and in order to gain information on the mechanism, we performed a series of experiments with silirene **1** at the catalytic and stoichiometric levels by combining catalysis and coordination chemistry. We were indeed able to isolate and fully characterize the first intermediate **I** derived from the activation of the silirene and study its fate upon reaction with an alkyne by multinuclear NMR spectroscopy. In addition, extensive DFT calculations enabled us to explain and corroborate our results, providing a better description of the elementary steps, the nature of the higher-energy intermediates, and ultimately the whole process.

RESULTS AND DISCUSSION

Palladium-Catalyzed Reaction with Silirene 1 and Acetylene. The reactivity of silirenes with alkynes under palladium-catalyzed conditions is intimately associated with steric factors, and their behavior strongly depends on the substitution pattern both at the silicon and at the carbon atoms of the three-membered ring heterocycle but also on the alkyne involved in the reaction.[19] In that respect, silirene **1** does not evolve in solution in the presence of $[Pd(PPh_3)_4]$, even upon prolonged heating at 100 °C. *Si,Si*-Di-*tert*-butyl silirenes[16,20] display enhanced kinetic stability, and no disilacyclohexadiene compounds of type **A** resulting from the silirene [3 + 3]-cyclodimerization[21] [Scheme 2—route (1)] could be observed in our case. This trend was confirmed by the reaction of **1** with acetylene (1 bar) under catalytic conditions. In that case, neither disilacyclohexadiene compounds **B** [Scheme 2—route (4)] nor bicyclic compounds of type **C** [Scheme 2—route (5)] as in the case of 1,1-dimethyl-2,3-bis(trimethylsilyl)silirene were detected.[18] The corresponding silole **2** was obtained as the sole product (Figure 1) and isolated in 80% isolated yield after purification by flash chromatography on silica gel. Single crystals of **2** could be obtained from a saturated pentane solution at room temperature, and their structure was determined by X-ray diffraction analysis.

Steric and Electronic Effects of the Alkyne on the Annulation Reaction. The influence of both the steric and the electronic nature of the terminal alkyne substrate was also investigated in order to get insight into the mechanism and to explain the exclusive chemo and regioselectivity observed with **1**. First, this study suggests that steric factors play a more prominent role than we initially thought in our case. This could be confirmed by the reaction of *tert*-butylacetylene and trimethylsilylacetylene that bear quaternary substituents directly linked to the triple bond. While the two substrates revealed total unreactivity under the standard catalytic conditions, the *tert*-butyl substituted silole **3** could be finally formed selectively under forcing conditions (100 °C, 72 h., cat. loading 10 mol %) and isolated in 82% yield after column chromatography on silica gel (Figure 2). **3** could be fully characterized by NMR, HRMS, as well as X-ray diffraction analyses.

In a second stage, the electronic effects of the alkyne substituents on the catalytic process were assessed by using different para-substituted ethynylbenzenes R−pC_6H_4−C≡C−

https://doi.org/10.1021/acs.inorgchem.3c00045
Inorg. Chem. XXXX, XXX, XXX−XXX

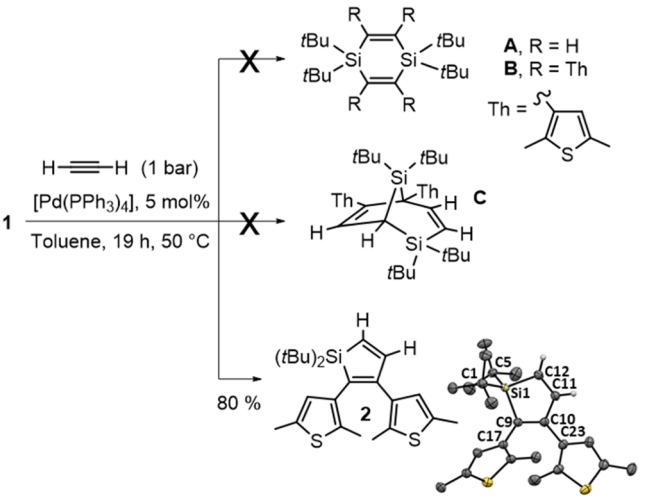

Figure 1. Reactivity of **1** with acetylene under Pd-catalyzed conditions, giving silole **2**, and X-ray structure of **2** with a displacement ellipsoid plot at a 50% probability level; non-vinylic hydrogens are omitted for clarity. Selected bond lengths [Å] and angles [°]: Si1−C12 1.872(2), Si1−C9 1.9005(19), C11−C12 1.343(3), C10−C11 1.491(3), C9−C10 1.369(3), C9−C17 1.474(3), C10−C23 1.477(3); C1−Si1−C9 115.53(9), C1−Si1−C5 116.62(9), C1−Si1−C12 108.51(9), C5−Si1−C9 109.74(8), C5−Si1−C12 111.91(9), C9−Si1−C12 91.86(9).

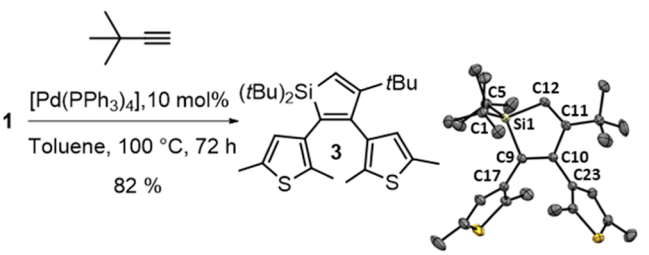

Figure 2. Synthesis of silole **3** by Pd-catalyzed annulation of **1** and *tert*-butylacetylene under forcing conditions (left). X-ray structure of **3** (right) with a displacement ellipsoid plot at a 50% probability level; hydrogen atoms are omitted for clarity. Selected bond lengths [Å] and angles [°]: Si1−C9 1.8871(18), Si1−C12 1.8537(19), C9−C10 1.359(2), C10−C11 1.528(2), C11−C12 1.349(3), C9−C17 1.485(2), C10−C23 1.491(2); C1−Si1−C9 113.17(8), C1−Si1−C5 116.98(8), C1−Si1−C12 106.41(8), C5−Si1−C9 111.67(8), C5−Si1−C12 114.81(9), C9−Si1−C12 90.84(8).

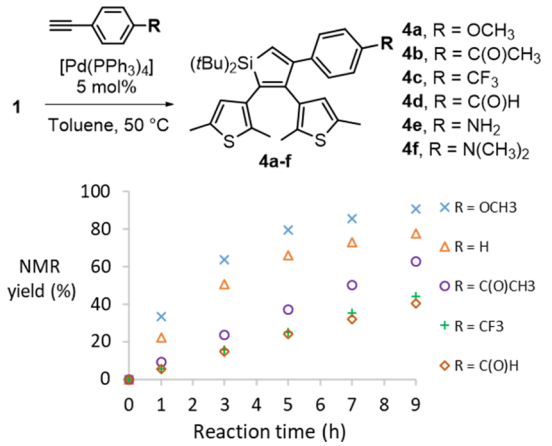

Figure 3. Synthesis of siloles **4a−f** by Pd-catalyzed annulation of para-substituted phenylacetylenes with **1** (top) and the plot of the catalytic transformations over time (down) for R = OCH_3, H, $C(O)CH_3$, CF_3, and C(O)H monitored by ^1H NMR spectroscopy (C_6D_6, internal standard DCE).

H (Figure 3, top). As previously reported, the catalytic transformation is tolerant to various functional groups, and we were pleased to observe the full conversion to aryl-substituted siloles **4a−f** that were isolated in quantitative yield, except **4d** (22% isolated yield) due to its degradation over silica gel during the purification step. They were all characterized by multinuclear NMR spectroscopy and HRMS analysis (see S6−S9). The NMR monitoring of the reaction shows that electron-rich substrates react faster, with the following tendency: −OMe > −H > −C(O)CH3 > −C(O)H ∼ $-CF_3$ (Figure 3, bottom).[22]

To gain further information on the mechanism of the reaction and more particularly on the coordination of the alkyne to the palladium in the catalytic process, the kinetic isotope effect (KIE) associated with a possible C−H bond cleavage of the alkyne moiety was evaluated. The study was conducted independently with protio and deutero phenylacetylene, Ph−C≡C−H, and Ph−C≡C−D, respectively, affording the previously described silole **5** and its isotopomer **5-D** (Scheme 4). No KIE could be observed from the rate of formation, suggesting that acetylenic C−H bond cleavage either does not occur at all or is not involved in the rate-determining step of the reaction. Additionally, and as observed by the group of Palmer and Woerpel, the reaction is clearly limited to terminal alkynes.[16a]

Scheme 4. Control Experiments of 1 with Protio-, Deutero-phenylacetylene, and 1-Phenyl-1-propyne

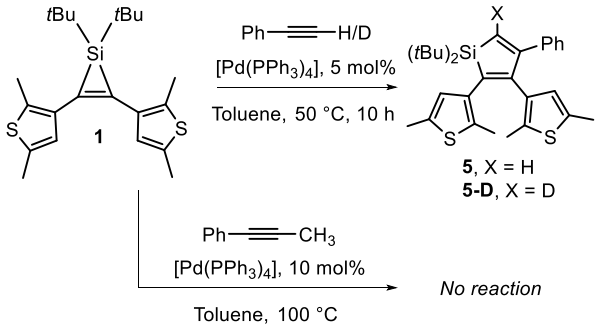

Our attempts to react **1** with 1-phenyl-1-propyne left the starting materials unchanged even under forcing conditions (Scheme 4, bottom).

OA of Palladium to Silirene 1. At that stage, we turned to coordination chemistry studies in order to address the question of palladasilacycles of type **I** (Scheme 3) in the palladium-catalyzed annulation reaction. 1,2-metallasilacyclobutenes are organometallic complexes with an unsaturated four-membered cyclic structure where a transition metal center is stabilized by two sigma bonds of different nature, σ-C−M and σ-Si−M, respectively. Although often invoked,[6c,16b,23] these complexes are rare and limited in number. A first description was reported by Ishikawa[24] in the case of nickelasilacyclobutene **C** generated from a silirene and $[(PEt_3)_4Ni(0)]$ (Figure 4).

It revealed instability and was only characterized in situ by NMR spectroscopy. Since then, other examples have appeared (**D**, $\mathbf{E^R}$, and $\mathbf{F^R}$),[25] but only four of them have been structurally characterized so far in the case of Pt (**D**), Ti ($\mathbf{E^H}$), and Ni ($\mathbf{F^H}$ and $\mathbf{F^{CH2OMe}}$) (Figure 4). They are either obtained by the [2 +

https://doi.org/10.1021/acs.inorgchem.3c00045
Inorg. Chem. XXXX, XXX, XXX−XXX

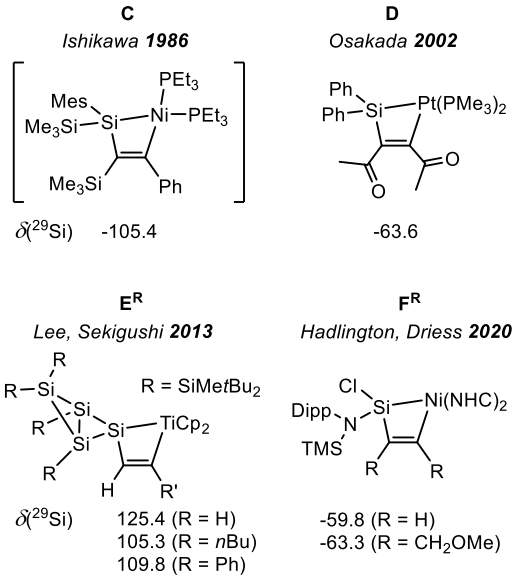

Figure 4. Previously described 1,2-metallasilacyclobutenes **C**−**F** and corresponding ^{29}Si NMR of the Si−M silicon nucleus.

2]-cycloaddition of the Si═M bond of a terminal silylene (M = Ni, Ti) with the C≡C triple bond of an alkyne or, in the case of Pt, by ring closure involving a γ-Si−H bond activation from a 3-sila-1-propenyl(silyl)platinum precursor and silane elimination. After perusal of the literature, we first assumed that 1,2-palladasilacyclobutenes should be accessed by OA of an adapted palladium precursor to silirene **1**. We first started to study the reactivity of silirene **1** with low-coordinated palladium (0) complexes $[(PR_3)_2Pd]$ (R = *t*Bu, *o*Tol) that are known to easily undergo OA reactions (Scheme 5).

Scheme 5. Preparation of 6-P(*t*Bu)$_3$ and 6-P(*o*Tol)$_3$ by Reaction of 1 and $[Pd(PR_3)_2]$

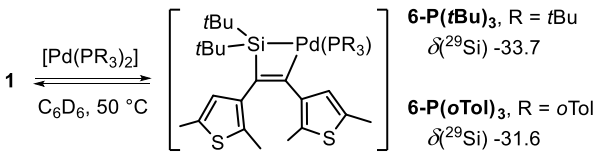

The reaction monitoring at 50 °C by ^{31}P{^{1}H} NMR of **1** with both complexes independently revealed the appearance of a new species displaying a resonance signal at δ 80.9 (R = *t*Bu) and δ 25.3 (R = *o*Tol) in addition to the remaining starting materials. The conversion to the product was estimated to be 40% and 82% for R = *t*Bu and R = *o*Tol, respectively.[26] In the ^{29}Si{^{1}H} NMR spectrum, new singlet resonance signals at δ −33.7 (R = *t*Bu) and δ −31.6 (R = *o*Tol), low field shifted regarding the starting material (δ −69.9), were observed. Except for the special case of titanasilacyclobutenes **E**^{R} that exhibit a peculiar deshielded signal for the Ti-bound Si atom, the observed values are downfield shifted compared to the values from the other group 10 metallacyclobutenes **C**, **D**, and **F**^{R} (Figure 4).[27] This feature could be attributed to the nature of the exocyclic silicon SiRR' substituents. Despite this discrepancy, the spectroscopic data from the full NMR characterization are consistent with a 1,2-palladacyclobutene structure for **6-P*t*Bu$_3$** and **6-P(*o*Tol)$_3$** with a monophosphine-coordinated palladium center. Unfortunately, attempts to isolate any of the two compounds by crystallization gave solid $Pd(PR_3)_n$ (*n* = 2, 3) complexes. NMR analysis of the mother liquors revealed only the presence of **1** in solution with minor decomposition products. This result is in agreement with previous NMR spectroscopic analyses (vide supra) and again suggests that the OA process leading to **6-P*t*Bu$_3$** and **6-P(*o*Tol)$_3$** is an equilibrated process. In view of these results, we reasoned that the excess phosphine ligand in solution could be the cause of the difficulties encountered in isolating complex **6**. We hypothesized that this point could be circumvented by the use of a "phosphine-free" palladium(0) precursor in the presence of a stoichiometric amount of a chosen phosphine.

We then turned to the use of the thermally unstable $[(COD)Pd(CH_2TMS)_2]$ dialkyl complex[28] as the convenient precursor of the active 14 electron [(COD)Pd] transient complex by simple reductive elimination of $(TMS-CH_2)_2$ (Figure 5, top).[29] A clean reaction occurs between **1** and

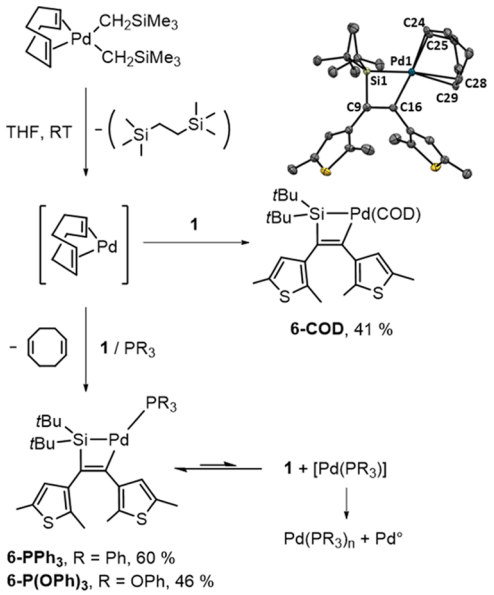

Figure 5. Decomposition of $[(COD)PdR_2]$ to [(COD)Pd] and its reactivity with (i) **1** affording **6-COD** (right) and (ii) **1** and PR_3 (R = Ph, OPh) affording **6-PPh$_3$** and **6-P(OPh)$_3$** (bottom). X-ray structure of **6-COD** (top right) with a displacement ellipsoid plot at a 50% probability level; hydrogen atoms are omitted for clarity. Selected bond lengths [Å] and angles [°]: Pd1−C24 2.309(3), Pd1−C25 2.351(2), Pd1−C28 2.454(3), Pd1−C29 2.510(3), Pd1−Si1 2.3237(9), Pd1−C16 2.064(3), Si1−C9 1.859(3), C9−C16 1.352(4); Si1−C9−C16 91.54(18), C9−C16−Pd1 116.37(18), C16−Pd1−Si1 63.75(8).

$[(COD)Pd(CH_2TMS)_2]$ in THF at room temperature (Figure 5, right), as shown by the ^{1}H NMR monitoring and the appearance of a singlet resonance signal at δ −34.8 in the ^{29}Si{^{1}H} NMR in agreement with the values obtained in the case of **6-P*t*Bu$_3$** and **6-P(*o*Tol)$_3$**. After work-up, **6-COD** could be isolated as colorless crystals in 41% yield, and its structure was determined by X-ray diffraction analysis. In the solid state, the palladium is in a distorted square-planar environment with an acute C16Pd1Si1 angle of 63.75(8)° [Σ_α(LPdL) = 360°]. The Si1Pd1 distance of 2.3237(9) Å is in the range of previously characterized silyl palladium(II) complexes (2.25−2.43 Å). Within the four-membered metallacycle, the C9Si1 bond of 1.859(3) Å is slightly elongated relative to the endocyclic Si−C bonds in **1** (1.82 Å in average), whereas the Si1C16 distance of 2.327(3) Å largely exceeds the sum of

https://doi.org/10.1021/acs.inorgchem.3c00045
Inorg. Chem. XXXX, XXX, XXX−XXX

covalent radii of the two atoms (1.84 Å, R = 1.26), confirming the cleavage of this bond. The C═C double bond length of 1.352(4) Å is identical to that in **1** [1.352(2) Å] with the exocyclic thienyl groups in an antiparallel conformation as in DTE derivatives.[30] The geometry around the C9 olefinic carbon atom deviates strongly from the ideal sp^2 arrangement with an acute C16C9Si1 angle of 88.09(9)°. This particular feature is more pronounced than in the case of the heavier platinum derivative **D** (97.8(5)°) but comparable to the case of the lighter nickel complexes **F** (average of 89.3°).

Following a similar synthetic strategy, **1** can be treated with $[(COD)Pd(CH_2TMS)_2]$ in the presence of a stoichiometric amount of phosphine ligands, leading to the exchange of the cyclooctadiene ligand (Figure 5, bottom). With one equivalent of Ph_3P or $(PhO)_3P$, the monophosphine complexes **6-PPh$_3$** and **6-P(OPh)$_3$** could be obtained in 65 and 46% yield, respectively, and fully characterized by NMR spectroscopy. The NMR spectra of **6-PPh$_3$** and **6-P(OPh)$_3$** are contaminated with a small amount of palladium(0) phosphine complexes $Pd(PR_3)_n$ (R = Ph, OPh), as well as silirene **1** (~5%). This can be explained by the existence of an equilibrium between **6-PPh$_3$** and **6-P(OPh)$_3$** and their reductive elimination products **1** and $[Pd(PR_3)]$ that lead to the slow decomposition of **6-PPh$_3$** and **6-P(OPh)$_3$** and the release of Pd° (Figure 5).[31] For the two complexes **6-PPh$_3$** and **6-P(OPh)$_3$**, the ^{29}Si NMR display a resonance signal at a similar chemical shift (**6-PPh$_3$** δ −27.2, **6-P(OPh)3** δ −26.9) and as a doublet due to scalar coupling to the ^{31}P nucleus ($^2J_{SiP}$ = 2.1 Hz, **6-PPh$_3$**; $^2J_{SiP}$ = 4.7 Hz, **6-P(OPh)$_3$**), indicative of the expected P−Pd−Si connectivity. Single crystals of **6-P(OPh)$_3$** suitable for X-ray diffraction analysis were grown at −30 °C from a saturated pentane/THF solution and their X-ray structure determined at 150 K (Figure 6).

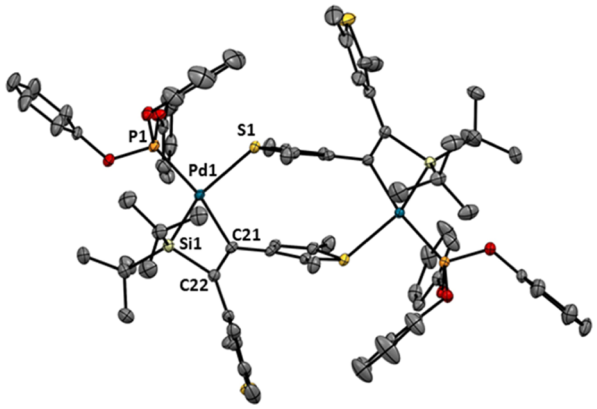

Figure 6. X-ray structure of **6-P(OPh)$_3$** with a displacement ellipsoid plot at a 50% probability level; hydrogen atoms are omitted for clarity. Selected bond lengths [Å] and angles [°]: Pd1−C21 2.085(2), Pd1−Si1 2.3380(7), Pd1−S1 2.6384(7), Pd1−P1 2.2548(7), Si1−C22 1.857(2), C22−C21 1.362(3); P1−Pd1−S1 104.38(2), C21−Pd1−S1 100.47(7), C21−Pd1−Si1 64.42(7), P1−Pd1−Si1 104.38(2), C21−C22−Si1 93.41(16).

In the solid state, it displays a dimeric structure revealing an intermolecular thienyl-to-palladium S → Pd coordination [Pd1S1 2.6384(7) Å; Pd2S3 2.6438(7) Å] with the thienyl ligand in *trans*-position to the silyl ligand. The 1,2-palladasilacyclobutene four-membered ring of **6-P(OPh)$_3$** exhibits similar geometric features as those of **6-COD**. To further explore the catalytic cycle, we continued by assessing the reactivity of the palladacycles with terminal alkynes in stoichiometric experiments (Scheme 6).

Scheme 6. Reactivity of Metallasilacyclobutene 6-L (L = PPh$_3$, P(OPh)$_3$, and COD) with Phenyl Acetylene

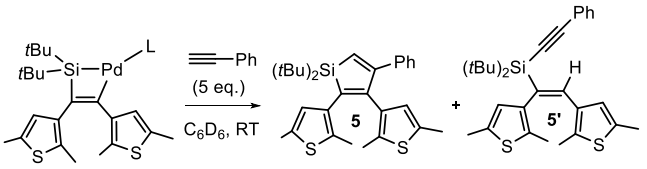

6-PPh$_3$, L = PPh_3	100	0
6-P(OPh)$_3$, L = $P(OPh)_3$	100	0
6-COD, L = COD	61(50)	39(28)

Both complexes **6-PPh$_3$** and **6-P(OPh)$_3$** react readily with phenylacetylene at room temperature ($t \approx 5$ and 30 min, respectively) to form selectively the model silole **5** as observed in the implemented catalytic conditions. Interestingly, the same reaction with **6-COD** is much slower and gives a mixture of **5** and an acyclic structural isomer **5′** in 50 and 28% isolated yield, respectively (see S20 for details). The structure of **5′** was determined thanks to HRMS and multinuclear NMR analyses. In particular, the $^3J_{SiH}$ coupling constant of 6.9 Hz indicates that the central olefin has retained its stereochemistry with the thienyl groups in the cis position.[32]

These results strongly support the involvement of a monophosphine-ligated 1,2-palladasilacyclobutene key intermediate in the palladium-catalyzed annulation reaction. With the objective of detecting intermediates derived from the palladacycle, the reaction between **6-PPh$_3$** and phenyl acetylene was monitored by NMR, at low temperature, in CD_2Cl_2. At 203 K, the ^{1}H NMR revealed the presence of resonance signals attributed to the model silole **5**[33] together with the remaining **6-PPh$_3$** in a 1.33:1 ratio. Besides remaining **6-PPh$_3$**, the ^{31}P NMR spectra exhibit an AB spin system with a coupling constant ($^2J_{PP}$ = 18.4 Hz) that is indicative of the presence of a Pd complex with two phosphines in the cis position. Based on multinuclear NMR 2D experiments (HMQC ^{1}H−^{31}P, HSQC, and HMBC ^{1}H−^{13}C) and after comparison to experimental data available in the literature,[34] the Pd(0)-alkyne π-complex $[(Ph_3P)_2Pd(\eta 2\text{-PhC}{\equiv}CH)]$ could be identified unambiguously (see S21−S25). It most likely results from ligand redistribution after the release of the silole ring between residual $[Pd(PPh_3)_n]$ and the excess of phenylacetylene present in the medium. This experiment clearly shows that the elementary steps occurring in the catalytic cycle after the formation of the 1,2-palladasilacyclobutene intermediate by OA require only little kinetic energy in the case of phenylacetylene. In that respect, the instability of 1,4-palladasilacyclohexadiene (type **II** species, Scheme 3) toward reductive elimination and silole formation is reminiscent of the behavior of nickel analogues,[25d] contrary to the platinum ones that proved stable at room temperature.[25b]

Theoretical Insight into the Reaction Mechanism. In order to get more insights into the reaction mechanism, DFT calculations at the B3PW91 level of theory have been performed, and the corresponding enthalpy profile computed with silirene **1** and phenylacetylene is shown in Figure 7 (for the Gibbs free energy profile, see Figure S127 in the Supporting Information).

https://doi.org/10.1021/acs.inorgchem.3c00045
Inorg. Chem. XXXX, XXX, XXX−XXX

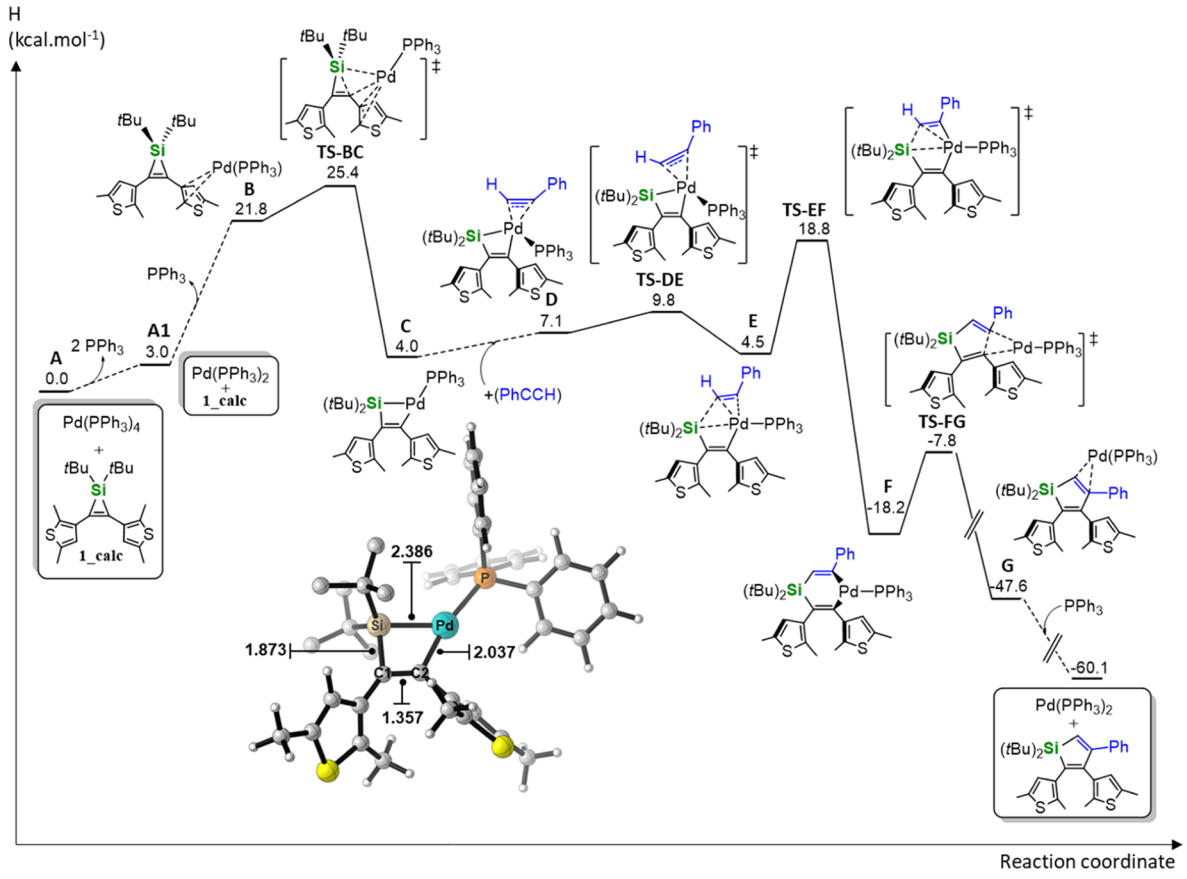

Figure 7. DFT-computed enthalpy profile (kcal mol^{-1}) of the Pd-catalyzed annulation reaction of phenylacetylene with silirene **1**; optimized structure of **C** and bond lengths within the Si−C−C−Pd metallacycle.

Phosphine Dissociation. Since the $[Pd(PPh_3)_4]$ compound is electronically saturated, the first step consists in the release of phosphine ligands to generate a reactive species. In order to evaluate the lability of the phosphine ligands bound to the Pd center, we computed the PPh_3 dissociation energy starting from $Pd(PPh_3)_4$. As shown in Figure 8, the dissociation of one, two, and three PPh_3 ligands displays a ΔH of −4.1, +3.0, and +37.7 kcal mol^{-1} (ΔG of −22.1, −32.8, and −9.1 kcal mol^{-1}), respectively, indicating that the starting $Pd(PPh_3)_4$ compound spontaneously loses two PPh_3 ligands in solution to afford the $Pd(PPh_3)_2$ species (**A1** in Figure 7), which is in line with literature data.[35] The replacement of the third phosphine by silirene **1** to form **B** is an energetically costly step (21.8 kcal mol^{-1}), which prepares the following OA reaction.

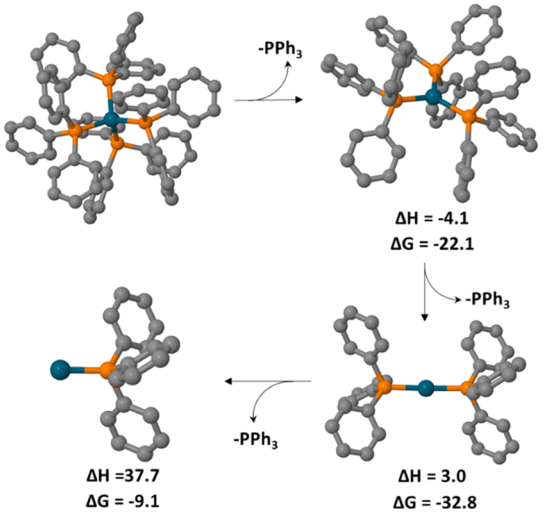

Figure 8. DFT-computed enthalpy and Gibbs free energy values for the PPh_3 dissociation reaction starting from the $Pd(PPh_3)_4$ compound. The ΔH and ΔG values refer to the starting $Pd(PPh_3)_4$ compound.

OA and 1,2-Palladasilacyclobutene Formation. In accordance with the experimental results reported above for the synthesis of **6-P*t*Bu$_3$** and **6-P(*o*Tol)$_3$**, the 1,2-palladasilacyclobutenes species **C** (**6-PPh$_3$**) is in equilibrium with the in situ-formed $Pd(PPh_3)_2$ species **A1**, with the displacement of the equilibrium toward the OA product **C** requiring thermal conditions (50 °C), given the presence of a large amount of free phosphine in solution. This OA reaction involves an early transition state where the C−Si bond is only slightly elongated with a low associated barrier of 3.6 kcal mol^{-1} (**TS-BC**) compared to **B**. For comparison purposes, the possibility of a first step involving the reaction between Pd(0) and the terminal alkyne was also considered (see Figure S128 in the Supporting Information). Starting from a diphosphine palladium (0) π-complex $[(Ph_3P)_2Pd(\eta^2\text{-PhC}{\equiv}CH)]$ **H**, the OA of the C−H bond to form the palladium (II) hydride $[(Ph_3P)_2Pd(C{\equiv}CPh)\ (H)]$ was, however, revealed to be highly endothermic (18.0 kcal mol^{-1}) with an associated kinetic barrier of 19.9 kcal mol^{-1} (**TS-HI**). This unfavorable step and the failure to localize the subsequent intermediates

https://doi.org/10.1021/acs.inorgchem.3c00045
Inorg. Chem. XXXX, XXX, XXX−XXX

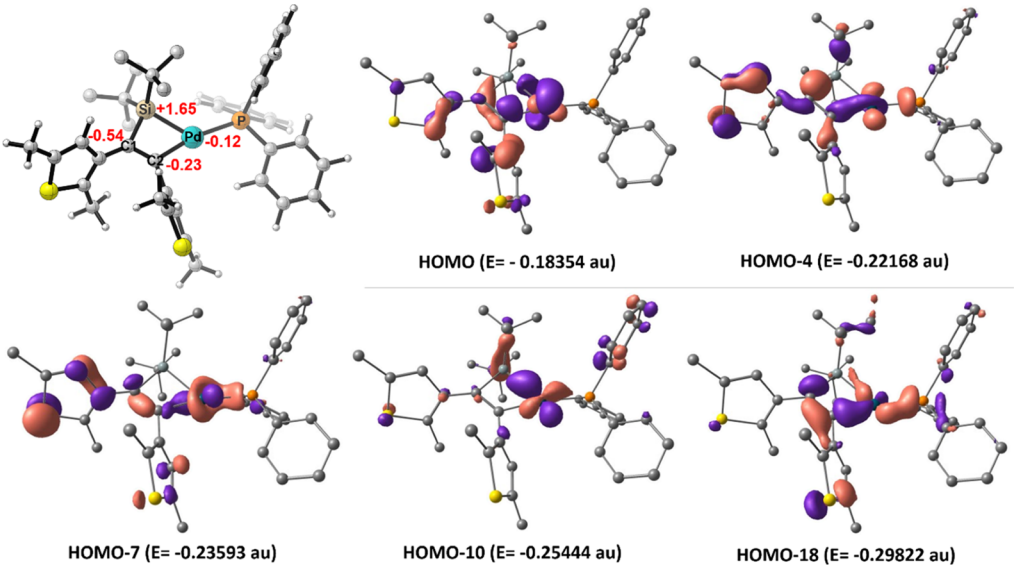

Figure 9. Geometry, NPA charge analysis, and representative MOs of the 1,2-metallasilacyclobutene **C** (isodensity value = 0.05 au).

made us rule out this alternative option. Due to its peculiar structure, the OA product **C** has been analyzed in more detail.

1,2-Palladasilacyclobutene Scaffold. As shown in Figure 7, the 1,2-palladasilacyclobutene **C** compound (**6-PPh$_3$**) displays a distorted T-shape environment around palladium with an acute C2PdSi angle of 60.69°. The SiPd distance (2.386 Å) is slightly longer than that measured experimentally for **6-COD** (2.3237(9) Å) and **6-P(OPh)$_3$** (2.3380(7) Å) but still within the range of previously characterized silyl palladium(II) complexes (2.25−2.43 Å). Within the four-membered metallacycle, the C1−Si bond length of 1.873 Å is slightly elongated with respect to the endocyclic Si−C bonds of the computed silirene compound **1_calc** (1.844 Å), whereas the C2Si distance of 2.255 Å largely exceeds the sum of covalent radii of the two atoms (1.84 Å, R = 1.26 Å). The C=C double bond length (1.357 Å) is identical to the one obtained for the computed silirene molecule (1.359 Å). The geometry around the C1 olefinic carbon atom is highly constrained, displaying an acute C2C1Si angle of 87.0°. To explore in depth the nature of the bonds involved in the Si−C−C−Pd cycle, we performed a NPA charge and MO analysis of **C** (Figure 9).

The computed natural charges indicate a positive charge of 1.65 for the electropositive Si center, together with a slight polarization of the C1−C2 bond, with the C1 carbon carrying a more negative charge (−0.54) than the C2 carbon (−0.23). The computed molecular orbitals responsible for the bonding within the Si−C1−C2−Pd cycle are shown in Figure 8. The HOMO, HOMO-4, HOMO-7, HOMO-10, and HOMO-18 orbitals describe the sigma bonding system of the four-membered 1,2-palladasilacyclobutene skeleton[36,37] (Figure 8), whereas the HOMO-1 and the HOMO-17 orbitals account for the π interaction between C1 and C2 (see Figure S129 in the Supporting Information). No orbital overlapping is detected between the Si and C2 atoms, despite the large SiC2 distance observed experimentally in the X-ray structures of **6** (vide supra), ruling out any possibility of bonding between these two centers.

Alkyne Insertion Process. From **C** (**6-PPh$_3$**), the alkyne may then insert into the Pd−Si bond of the metallacycle to form the 1,4-palladasilacyclohexadiene species. The process occurs in three steps, involving (i) the coordination of the alkyne to **C**; (ii) the insertion of the alkyne into the Pd−Si bond with the retention of the Pd−Si bond (**TS-DE**), and (iii) the breaking of the Pd−Si bond (**TS-EF**) to afford the 1,4-palladasilacyclohexadiene species **F**. As shown in Figure 7, after the formation of **D**[38] via the endothermic coordination of the alkyne to **C** in a η^2 side-on fashion (7.1 kcal mol^{-1} with respect to the entrance channel **A**), the two-step insertion of the alkyne into the Pd−Si bond takes place through two kinetically accessible barriers of 9.8 and 18.8 kcal mol^{-1}. The alternative scenario involving the alkyne insertion into the Pd−C bond has been excluded due to its unreasonably high kinetic barrier of 39.6 kcal mol^{-1} (see Figures S132 and S133 in the Supporting Information). The resulting 1,4-palladasilacyclohexadiene species **F** is exothermic by −18.2 kcal mol^{-1} and represents the driving force of the reaction. Two regioisomers are possible depending on whether the terminal alkyne carbon binds the Si atom (Figure 7) or the Pd atom (see Figures S134 and S135 in Supporting Information). As shown in Figures 7 and S134 in the Supporting Information, the formation of the regio-isomer displaying the terminal alkyne carbon bonded to the Si atom is more favorable, both kinetically and thermodynamically (**TS-DE** = 9.8 kcal mol^{-1}; **TS-EF** = 18.8 kcal mol^{-1}; **F** = −18.2 kcal mol^{-1} vs **TS-D1E1** = 28.6 kcal mol^{-1}; **TS-E1F1** = 32.3 kcal mol^{-1}; **F1** = −12.4 kcal mol^{-1}); the steric repulsion between the *t*Bu groups at the Si center and the phenyl substituent of the alkyne plays an important role.

Reductive Elimination Step. From species **F** in Figure 7, an easy reductive elimination process may then occur with a kinetic barrier of 10.4 kcal mol^{-1}, leading to the exothermic formation of the experimentally observed silole product (**G** = −47.6 kcal mol^{-1}). The relative orientation of the two thienyl substituents is likely to play an important role when tetracoordinate Pd species are involved. This is related to the well-known conformational preference of the DTE skeleton for two possible antiparallel orientations of the thienyl groups,[30] resulting in two possible diastereomeric structures when tetracoordinated Pd species are involved. As shown by the comparison between the enthalpy profiles in Figure 10 (see Figures S136 and S137 in the Supporting Information for the

https://doi.org/10.1021/acs.inorgchem.3c00045
Inorg. Chem. XXXX, XXX, XXX−XXX

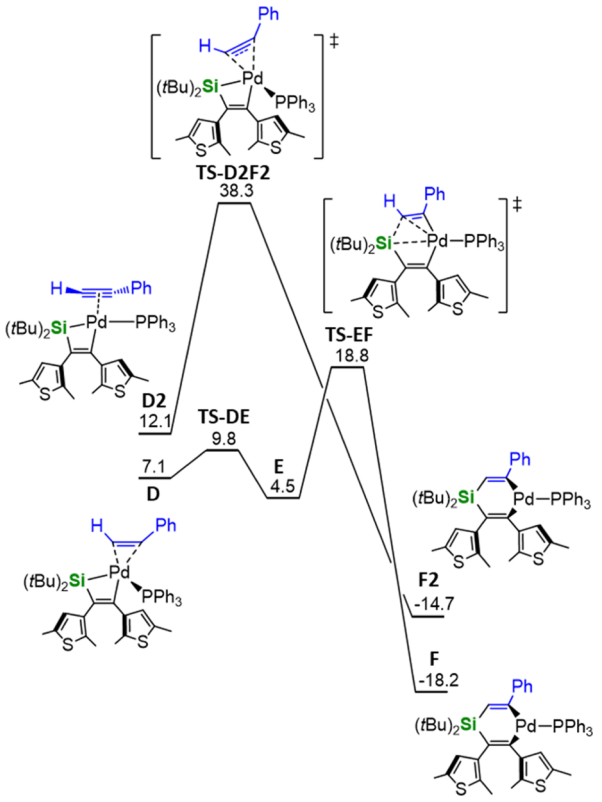

Figure 10. DFT-computed enthalpy profiles for the formation of 1,4-palladasilacyclohexadiene **F** from π-complex **D** with the two possible antiparallel orientation of the thienyl groups.

corresponding Gibbs free energy profiles), the different orientation of the thienyl groups particularly affects the alkyne insertion step.

Starting from the alkyne π-complex **D2**, indeed, the phenylacetylene insertion becomes a one-step process with an associated kinetic barrier of 38.2 kcal mol^{-1} (**TS-D2F2**), which cannot compete with the pathway starting from **D**, displaying a kinetic barrier of 18.8 kcal mol^{-1} (**TS-EF**).

Electronic and Steric Effects in the Insertion Step of the Alkyne. In line with the experimental observations, we computed the annulation reaction of different para-substituted ethynylbenzenes R−pC$_6$H$_4$−C≡C−H (R = CF$_3$ and OMe). As shown in Figures S138−S141 in the Supporting Information, compared to the phenylacetylene analogues, the energies of intermediates **D_CF3** and **D_OMe** differ by less than 2 kcal mol^{-1} (5.9 and 7.5 kcal mol^{-1}, respectively, compared to 7.1 kcal mol^{-1} for **D**) and the energies of alkyne insertion transition states, **TS-DE_CF$_3$**, **TS-EF_CF$_3$** and **TS-DE_OMe**, **TS-EF_OMe** by less than 4 kcal mol^{-1} (8.8 and 10.1 kcal mol^{-1} compared to 9.8 kcal mol^{-1} for **TS-DE** and 16.5 and 19.7 compared to 18.8 kcal mol^{-1} for **TS-EF**). According to the literature,[39] these values are of the same order of magnitude as the accuracy of the DFT method used here, indicating that the electronic effects of the alkyne substituents observed experimentally are too small to be rationalized by DFT methods. The same conclusion applies to the effect of PPh$_3$ and P(OPh)$_3$ phosphines. As shown in the comparison of the enthalpy profiles of the Pd-catalyzed annulation reaction of Ph−C≡C−H with silirene **1** in the presence of PPh$_3$ and P(OPh)$_3$ (Figure S142), the effect of phosphine on the reaction and, more particularly, on the stabilization of the intermediates is too small to allow a clear differentiation by means of DFT calculations. To further confirm the presence of one phosphine coordinated to the Pd center during the alkyne insertion process, we computed the phosphine dissociation from adduct **D** (**D4**) and the following PhCCH insertion reaction without the PPh$_3$ coordination. As shown in the enthalpy profile in Figure S143, while the phosphine dissociation from **D** to **D4** is athermic, the following PhCCH insertion becomes kinetically unfavorable, with the corresponding transition state enthalpy passing from 9.8 kcal mol^{-1} (**TS-DE**) to 36.4 kcal mol^{-1} (**TS-D4E4**). To get more insight into the steric factors, we also computed the annulation reaction of *tert*-butylacetylene (see Figures S144 and S145 in the Supporting Information). This time the energy of intermediate **D_*t*Bu** is significantly higher than that of intermediate **D** (11.3 vs 7.1 kcal mol^{-1}), and the formation of the 1,4-palladasilacyclohexadiene compound involves higher kinetic barriers (14.2 and 23.6 kcal mol^{-1} for **TS-DE_*t*Bu** and **TS-EF_*t*Bu** vs 9.8 and 18.8 kcal mol^{-1} for **TS-DE** and **TS-EF**). Compared to phenylacetylene, therefore, the more forcing conditions needed with *tert*-butylacetylene, (100 °C, 72 h., cat. loading 10 mol %) may be accounted for by both its more endothermic coordination and its less kinetically favorable insertion barriers.

CONCLUSIONS

In summary, this work contributes to a better understanding of the Pd-catalyzed silole synthesis from alkynes and silacyclopropenes in terms of scope, limitations, and mechanism. The influence of the alkyne substrate was first evaluated, revealing that the reaction is nicely functional group tolerant. When conducted under an acetylene atmosphere, no scrambling of the reagents is observed, with the corresponding silole being the sole product of the reaction. The steric and electronic environment at the alkyne group has a significant impact on the reaction kinetics: while electron-rich alkynes react faster, sterically hindered alkynes display considerably lower reaction rates. In particular, a slow reaction is observed with the bulky *t*Bu−C≡C−H whereas no reaction is detected in the case of Me$_3$Si−C≡C−H. From a mechanistic point of view, the question of the involvement in the process of the hitherto unknown 1,2-palladasilacyclobutene intermediate was duly addressed. Four monophosphine-coordinated **6-PR$_3$** (R = *o*Tol, *t*Bu, Ph, and OPh) and one cyclooctadiene-ligated **6-COD** 1,2-palladasilacyclobutene could be prepared and characterized by multinuclear NMR spectroscopy. The OA of Pd(0) precursors to silacyclopropene **1** was found to be equilibrated in all cases. The nature of the 1,2-palladasilacyclobutenes could be ultimately ascertained by the X-ray diffraction analysis of **6-P(OPh)$_3$** and **6-COD**. Under stoichiometric conditions, **6-PPh$_3$** reacts cleanly with phenylacetylene to afford the expected silole, thus strongly supporting the involvement of 1,2-palladasilacyclobutene as a key intermediate of the catalytic cycle. The putative 1,4-palladasilacyclohexadiene intermediate resulting from the alkyne insertion could not be observed, most likely due to fast reductive elimination and silole formation even at low temperatures. For greater rationalization, we carried out a DFT study on the involved reaction mechanism by computing different possible mechanistic pathways and comparing the theoretical data with the experimental ones. The computational results indicate that the Pd-catalyzed annulation reaction of alkynes with silirene **1** occurs in three main steps, involving

https://doi.org/10.1021/acs.inorgchem.3c00045
Inorg. Chem. XXXX, XXX, XXX−XXX

(i) the OA of Pd(0) to the silirene; (ii) the insertion of the alkyne into the Pd−Si bond; and (iii) the reductive elimination on the 1,4-palladasilacyclohexadiene compound with the exothermic release of the silole product. The starting $Pd(PPh_3)_4$ compound spontaneously evolves in solution to the $Pd(PPh_3)_2$ species as the prelude of the OA of silirene via the endothermic loss of an additional phosphine. The resulting 1,2-palladasilacyclobutene species **C** is in equilibrium with the in situ-formed $Pd(PPh_3)_2$ compound, with the displacement of the equilibrium toward the OA product requiring high thermal conditions (50 °C), given the presence of a large amount of free phosphine in solution. The subsequent alkyne insertion reaction occurs selectively into the Pd−Si bond of **C**, with the resulting 1,4-palladasilacyclohexadiene species displaying the terminal alkyne carbon bonded to the silicon atom. In accordance with the experimental results, therefore, the computational data confirm that the alkyne insertion is a chemo- and regio-selective reaction, with the formation of the experimentally observed silole strongly favored.

EXPERIMENTAL SECTION

General Considerations. Unless otherwise stated, all reactions and manipulations were carried out under an atmosphere of dry argon using standard Schlenk techniques or in a glovebox. CD_2Cl_2, C_6D_6, and THF d^8 were dried over calcium dihydride, distilled, and stored over 3 Å molecular sieves prior to use. Tetrahydrofuran was dried over calcium dihydride and distilled prior to use. All other solvents were purged with argon and dried using an MBRAUN solvent purification system. ^1H, ^{13}C, ^{31}P, and ^{29}Si NMR spectra were recorded on a Bruker Avance III 400 NMR spectrometer or a Bruker Avance III HD 500 NMR spectrometer. All ^{29}Si NMR spectra have been recorded with proton decoupling. Chemical shifts were expressed in positive signs, in parts per million, calibrated to residual ^1H (5.32 ppm for CD_2Cl_2, 7.16 ppm for C_6D_6, and 1.72 and 3.58 for THF d^8) and ^{13}C (53.84 ppm for CD_2Cl_2, 128.06 ppm for C_6D_6, and 25.31 and 67.21 for THF d^8), 85% H_3PO_4, and external tetramethylsilane solvent signals, respectively. Mass spectra were recorded on a MAXIS 4G or an Ultraflex III mass spectrometer. Elemental analyses were performed at the ScanMat-CRMPO on a Thermo Fisher Flash 1112 Series. Silirene **1**[17] and $[(COD)Pd(CH_2TMS)_2]$[29b] were prepared according to literature procedures.

Compound ***2***. A Schlenk tube loaded with a solution of silirene **1** (60.0 mg, 0.154 mmol) and palladium tetrakis(triphenylphosphine) (8.9 mg, 7.7×10^{-3} mmol, 5.0 mol %) in toluene (2 mL) was pressurized with acetylene (1 bar), and the resulting mixture was stirred for 19 h at 50 °C, giving a dark solution. The volatiles were then removed under reduced pressure, and the residue was then purified by column chromatography on silica gel (SiO_2 15 g, gradient: pentane 100% → pentane/DCM (95/5), R_f (pentane) = 0.52), giving the expected compound as a crystalline white solid in 80% yield. Single crystals suitable for X-ray diffraction studies were obtained from a saturated pentane solution at room temperature.

^1H NMR (CD_2Cl_2, 400 MHz): δ (ppm) 1.08 (s, 18H, C$\underline{H}_3$ *t*Bu), 1.66 (s, 3H, C$\underline{H}_3$−Th), 1.95 (s, 3H, C$\underline{H}_3$−Th), 2.32 (s, 3H, C$\underline{H}_3$−Th), 2.38 (s, 3H, C$\underline{H}_3$−Th), 6.18 (d, 1H, $^3J_{HH}$ = 10.5 Hz, Si−C$\underline{H}$), 6.36 (s, 1H, $\underline{H}$ Th), 6.63 (s, 1H, $\underline{H}$ Th), 7.09 (d, 1H, $^3J_{HH}$ = 10.5 Hz, Si−C(H)=C$\underline{H}$); $^{13}C\{^1H\}$ NMR (CD_2Cl_2, 100 MHz): δ (ppm) 14.3 (s, $\underline{C}H_3$−Th), 14.7 (s, $\underline{C}H_3$−Th), 15.2 (s, $\underline{C}H_3$−Th), 15.4 (s, $\underline{C}H_3$−Th), 19.7 (s, $\underline{C}$ *t*Bu), 29.1 (s, $\underline{C}H_3$ *t*Bu), 126.6 (s, $\underline{C}$H Ph), 126.9 (s, $\underline{C}$H Th), 129.7 (s, Si−$\underline{C}$H), 130.0, 133.4, 135.4, 135.5, 135.7, 137.8, 138.0 and 148.9 (s, $\underline{C}$quat.), 152.0 (s, Si−C(H)=$\underline{C}$H); ^{29}Si NMR (CD_2Cl_2, 79 MHz): δ (ppm) 21.8 (s). HRMS (ESI, CH_2Cl_2) calcd for $[C_{24}H_{34}SiS_2]^+$, 414.18657; found, 414.1866 (0 ppm).

Compound ***3***. To a solution of silirene **1** (50.0 mg, 0.129 mmol) and 3,3-dimethyl-but-1-yne (79.2 μL, 0.643 mmol, 5.00 equiv) in C_6D_6 (0.65 mL) was added tetrakis(triphenylphosphine) palladium (0) (14.9 mg, 1.29×10^{-2} mmol, 10.0 mol %) under stirring, and the resulting mixture was stirred for 3 days at 100 °C, giving a bright yellow mixture. The solution was concentrated to dryness, and the residue was purified by column chromatography on silica gel [SiO_2 15 g, eluent petroleum ether (100%), R_f = 0.60], giving the expected compound as a white solid in 82% yield. Single crystals suitable for X-ray diffraction were obtained from a saturated solution of pentane at −30 °C.

^1H NMR (CD_2Cl_2, 400 MHz): δ (ppm) 0.99 (s, 9H, C$\underline{H}_3$ Si*t*Bu), 1.05 (s, 9H, C$\underline{H}_3$ *t*Bu), 1.18 (s, 9H, C$\underline{H}_3$ Si*t*Bu), 2.01 (s, 3H, C$\underline{H}_3$−Th), 2.05 (s, 3H, C$\underline{H}_3$−Th), 2.30 (s, 3H, C$\underline{H}_3$−Th), 2.33 (s, 3H, C$\underline{H}_3$−Th), 5.94 (s with ^{29}Si sat., 1H, $^2J_{HSi}$ = 10.5 Hz, $\underline{H}$ vinyl), 6.41 (s, 1H, $\underline{H}$ Th), 6.51 (s, 1H, $\underline{H}$ Th); $^{13}C\{^1H\}$ NMR (CD_2Cl_2, 100 MHz): δ (ppm) 14.7 (s, $\underline{C}H_3$−Th), 15.1 (s, $\underline{C}H_3$−Th), 15.3 (s, $\underline{C}H_3$−Th), 15.7 (s, $\underline{C}H_3$−Th), 19.6 (s, $\underline{C}$ Si*t*Bu), 19.9 (s, $\underline{C}$ Si*t*Bu), 28.9 (s, $\underline{C}H_3$ Si*t*Bu), 29.5 (s, $\underline{C}H_3$ Si*t*Bu), 30.6 (s, $\underline{C}H_3$ *t*Bu), 37.2 (s, $\underline{C}$ *t*Bu), 121.4 (s, $\underline{C}$H vinyl), 126.6 (s, $\underline{C}$H Th), 128.6 (s, $\underline{C}$quat.), 129.0 (s, $\underline{C}$H Th), 132.5, 133.2, 134.7, 138.6 and 138.7 (s, $\underline{C}$quat.), 143.5 (s, C−Si), 154.6 (s, $\underline{C}$quat.), 171.4 (s, $\underline{C}$quat.). ^{29}Si NMR (C_6D_6, 79 MHz): δ (ppm) 13.3 (s). HRMS (ESI, CH_3OH/CH_2Cl_2 (90/10)) calcd for $[C_{28}H_{42}SiS_2+Na]^+$, 493.23894; found, 493.2394 (1 ppm); calcd for $[C_{28}H_{42}SiS_2+K]^+$, 509.21288; found, 509.2130 (0 ppm). Anal. Calcd for $[C_{28}H_{42}SiS_2]$; C, 71.42; H, 8.99; S, 13.62. Found: C, 71.60; H, 9.00; S, 13.16.

Compound ***4a−f****: General Procedure.* To a solution of silirene **1** (50.0 mg, 0.129 mmol) and alkyne (0.129 mmol, 1.00 equiv) in toluene (1.6 mL) was added palladium tetrakis(triphenylphosphine) (7.4 mg, 6.4×10^{-3} mmol, 5.0 mol %) under stirring, and the resulting mixture was stirred for 24 h at 50 °C, giving a bright yellow solution. The volatiles were then removed under reduced pressure giving an oily residue that was purified by column chromatography on silica gel (see underneath for chromatography conditions for each compound). These compounds were obtained in quantitative yield, but the aldehyde **4d** that partially decomposes on silica gel was isolated in only 22% yield.

Compound ***4a*** *(R = OMe).* After flash chromatography on silica gel {SiO_2, 15 g; gradient DCM/pentane (10/90) → DCM/pentane (20/80); R_f [DCM/pentane (20/80)] = 0.60}, the product was obtained as a white solid. Single crystals suitable for X-ray diffraction were obtained from a saturated diethylether solution at −20 °C.

^1H NMR (CD_2Cl_2, 400 MHz): δ (ppm) 1.09 (s, 9H, C$\underline{H}_3$ *t*Bu), 1.14 (s, 9H, C$\underline{H}_3$ *t*Bu), 1.74 (s, 3H, C$\underline{H}_3$−Th), 1.79 (s, 3H, C$\underline{H}_3$−Th), 2.20 (s, 3H, C$\underline{H}_3$−Th), 2.39 (s, 3H, C$\underline{H}_3$−Th), 2.89 (s, 3H, OC$\underline{H}_3$), 5.96 (s, 1H, $\underline{H}$ Th), 5.99 (s with ^{29}Si sat., 1H, $^2J_{HSi}$ = 11.2 Hz, $\underline{H}$ vinyl), 6.50 (d, 2H, $^3J_{HH}$ = 8.9 Hz, $\underline{H}$ Ph), 6.64 (s, 1H, $\underline{H}$ Th), 6.89 (d, 2H, $^3J_{HH}$ = 8.9 Hz, $\underline{H}$ Ph); $^{13}C\{^1H\}$ NMR (CD_2Cl_2, 100 MHz): δ (ppm) 14.5 (s, $\underline{C}H_3$−Th), 14.6 (s, $\underline{C}H_3$−Th), 15.2 (s, $\underline{C}H_3$−Th), 15.4 (s, $\underline{C}H_3$−Th), 19.9 (s, $\underline{C}$ *t*Bu), 20.1 (s, $\underline{C}$ *t*Bu), 29.1 (s, $\underline{C}H_3$ *t*Bu), 29.3 (s, $\underline{C}H_3$ *t*Bu), 40.7 (s, O$\underline{C}H_3$), 111.6 (s, $\underline{C}$H Ph), 126.0 (s, $\underline{C}$H vinyl), 127.2 (s, $\underline{C}$H Th), 128.1 (s, $\underline{C}$H Th), 128.7 (s, $\underline{C}$H Ph), 130.0 (s, $\underline{C}$ Th), 130.5 (s, $\underline{C}$ Ph), 133.1, 134.1, 135.1, 137.4 and 138.1 (s, $\underline{C}$−Th), 140.2 (s, $\underline{C}$−Si), 150.0 (s, $\underline{C}$ Ph), 151.4 (s, Si−CH = $\underline{C}$−Ph), 163.1 (s, Si−C=$\underline{C}$−Th); ^{29}Si NMR (CD_2Cl_2, 79 MHz): δ (ppm) 16.7 (s). HRMS (ESI, CH_3OH/CH_2Cl_2 (95/5)): calcd for $[C_{31}H_{40}SiOS_2+H]^+$, 521.23626; found, 521.2361 (0 ppm). Anal. Calcd for $[C_{31}H_{40}SiOS_2]$; C, 71.48; H, 7.74. Found: C, 71.36; H, 7.82.

Compound ***4b*** *(R = COMe).* After flash chromatography on silica gel [SiO_2, 15 g; gradient DCM/pentane (50/50) → DCM/pentane (70/30); R_f (DCM/pentane (50/50)) = 0.60], the product was obtained a clear yellow oil.

^1H NMR (CD_2Cl_2, 400 MHz): δ (ppm) 1.10 (s, 9H, C$\underline{H}_3$ *t*Bu), 1.16 (s, 9H, C$\underline{H}_3$ *t*Bu), 1.73 (s, 3H, C$\underline{H}_3$−Th), 1.79 (s, 3H, C$\underline{H}_3$−Th), 2.16 (s, 3H, C$\underline{H}_3$−Th), 2.39 (s, 3H, C$\underline{H}_3$−Th), 2.53 (s, 3H, C(O)C$\underline{H}_3$), 5.91 (s, 1H, $\underline{H}$ Th), 6.24 (s with ^{29}Si sat., 1H, $^2J_{HSi}$ = 10.7 Hz, $\underline{H}$ vinyl), 6.65 (s, 1H, $\underline{H}$ Th), 7.11 (d, 2H, $^3J_{HH}$ = 8.5 Hz, $\underline{H}$ Ph), 7.73 (d, 2H, $^3J_{HH}$ = 8.5 Hz, $\underline{H}$ Ph); $^{13}C\{^1H\}$ NMR (CD_2Cl_2, 100 MHz): δ (ppm) 14.5 (s, $\underline{C}H_3$−Th), 14.6 (s, $\underline{C}H_3$−Th), 15.1 (s, $\underline{C}H_3$−Th), 15.4 (s, $\underline{C}H_3$−Th), 20.0 (s, $\underline{C}$ *t*Bu), 20.1 (s, $\underline{C}$ *t*Bu), 26.8 (s, C(O)$\underline{C}H_3$), 29.0 (s, $\underline{C}H_3$ *t*Bu), 29.3 (s, $\underline{C}H_3$ *t*Bu), 127.0 (s, $\underline{C}$H Th), 127.6 (s, $\underline{C}$H Th), 127.7 (s, $\underline{C}$H Ph), 128.0 (s, $\underline{C}$H Ph), 130.3 (s, $\underline{C}$

https://doi.org/10.1021/acs.inorgchem.3c00045
Inorg. Chem. XXXX, XXX, XXX−XXX

Th), 131.5 (s, CH vinyl), 133.5 (s, C Th), 134.9 (s, C Th), 135.5 (s, C Th), 135.8 (s, C−C(O)CH_3), 136.6 (s, C Th), 137.6 (s, C Th), 140.8 (s, C−Si), 146.9 (s, C Ph), 150.1 (s, Si−CH = C−Ph), 162.4 (s, Si−C=C−Th), 197.9 (s, C=O); ^{29}Si NMR (CD_2Cl_2, 79 MHz): δ (ppm) 17.7 (s). HRMS (ESI, CH_2Cl_2): calcd for $[C_{32}H_{40}SiOS_2]^+$, 532.22844; found, 532.2283 (0 ppm). Anal. Calcd for $[C_{28}H_{42}SiS_2]$; C, 72.13; H, 7.57. Found: C, 72.41; H, 7.56.

Compound ***4c*** *(R = CF_3).* After flash chromatography on silica gel [SiO_2, 15 g; eluent, DCM/pentane (5/95); R_f = 0.8], the product was obtained as a white solid.

^{1}H NMR (CD_2Cl_2, 400 MHz): δ (ppm) 1.10 (s, 9H, CH_3 *t*Bu), 1.17 (s, 9H, CH_3 *t*Bu), 1.74 (s, 3H, CH_3−Th), 1.79 (s, 3H, CH_3−Th), 2.16 (s, 3H, CH_3−Th), 2.39 (s, 3H, CH_3−Th), 5.89 (s, 1H, H Th), 6.24 (s with ^{29}Si sat., 1H, $^2J_{HSi}$ = 10.6 Hz, H vinyl), 6.66 (s, 1H, H Th), 7.14 (d, 2H, $^3J_{HH}$ = 8.0 Hz, H Ph), 7.41 (d, 2H, $^3J_{HH}$ = 8.0 Hz, H Ph); ^{13}C{^{1}H} NMR (CD_2Cl_2, 100 MHz): δ (ppm) 14.5 (s, CH_3−Th), 14.6 (s, CH_3−Th), 15.1 (s, CH_3−Th), 15.4 (s, CH_3−Th), 20.0 (s, C *t*Bu), 20.1 (s, C *t*Bu), 29.0 (s, CH_3 *t*Bu), 29.3 (s, CH_3 *t*Bu), 124.5 (q, $^4J_{CF}$ = 3.8 Hz, CH Ph), 124.9 (q, $^1J_{CF}$ = 271.7 Hz, CF_3), 126.9 (s, CH Th), 127.6 (s, CH Th), 128.2 (s, CH Ph), 128.7 (q, $^2J_{CF}$ = 32.0 Hz, C-CF_3), 130.3 (s, C Th), 131.5 (s, CH vinyl), 133.5, 135.0, 135.5, 136.5 and 137.6 (s, C Th), 140.8 (s, C−Si), 145.9 (s, C Ph), 150.0 (s, Si−CH=C−Ph), 162.0 (s, Si−C=C−Th); ^{29}Si NMR (CD_2Cl_2, 79 MHz): δ (ppm) 17.7 (s); ^{19}F{^{1}H} NMR (CD_2Cl_2, 376 MHz): δ (ppm) −62.7 (s). HRMS (ESI, CH_2Cl_2): calcd for $[C_{31}H_{37}F_3SiS_2]^+$, 558.20526; found, 558.2053 (0 ppm). Anal. Calcd for $[C_{28}H_{42}SiS_2]$; C, 66.63; H, 6.67. Found: C, 66.97; H, 6.83.

Compound ***4d*** *(R = CHO).* After flash chromatography on silica gel [SiO_2, 15 g; eluent, pentane/ethyl acetate (97/3); R_f = 0.47], the product was obtained as a fluffy pale-yellow solid.

^{1}H NMR (CD_2Cl_2, 400 MHz): δ (ppm) 1.10 (s, 9H, CH_3 *t*Bu), 1.17 (s, 9H, CH_3 *t*Bu), 1.73 (s, 3H, CH_3−Th), 1.80 (s, 3H, CH_3−Th), 2.15 (s, 3H, CH_3−Th), 2.40 (s, 3H, CH_3−Th), 5.90 (s, 1H, H Th), 6.28 (s with ^{29}Si sat., 1H, $^2J_{HSi}$ = 10.6 Hz, H vinyl), 6.66 (s, 1H, H Th), 7.19 (d, 2H, $^3J_{HH}$ = 8.2 Hz, H Ph), 7.66 (d, 2H, $^3J_{HH}$ = 8.2 Hz, H Ph); ^{13}C{^{1}H} NMR (CD_2Cl_2, 100 MHz): δ (ppm) 14.1 (s, CH_3−Th), 14.2 (s, CH_3−Th), 14.7 (s, CH_3−Th), 15.0 (s, CH_3−Th), 19.6 (s, C *t*Bu), 19.7 (s, C *t*Bu), 28.5 (s, CH_3 *t*Bu), 28.9 (s, CH_3 *t*Bu), 126.5 (s, CH Th), 127.1 (s, CH Th), 128.1 (s, CH Ph), 128.7 (s, CH Ph), 129.9 (s, C Th), 131.6 (s, CH vinyl), 133.1, 134.5, 134.7, 135.1, 136.1 and 137.1 (s, C Th), 140.4 (s, C−Si), 147.9 (s, C Ph), 149.5 (s, Si−CH = C−Ph), 161.9 (s, Si−C=C−Th), 191.8 (s, C=O); ^{29}Si NMR (CD_2Cl_2, 79 MHz): δ (ppm) 17.8 (s). HRMS (ESI, CH_2Cl_2): calcd for $[C_{31}H_{38}OSiS_2]^+$, 518.21279; found, 518.2126 (0 ppm). Anal. Calcd for $[C_{28}H_{42}SiS_2]$; C, 71.76; H, 7.38. Found: C, 72.22; H, 7.26.

Compound ***4e*** *(R = NH_2).* After flash chromatography on silica gel [SiO_2, 15 g; eluent, DCM/pentane/methanol (20/79/1); R_f = 0.1], the product was obtained as an oil.

^{1}H NMR (CD_2Cl_2, 400 MHz): δ (ppm) 1.09 (s, 9H, CH_3 *t*Bu), 1.14 (s, 9H, CH_3 *t*Bu), 1.73 (s, 3H, CH_3−Th), 1.79 (s, 3H, CH_3−Th), 2.19 (s, 3H, CH_3−Th), 2.38 (s, 3H, CH_3−Th), 3.64 (s br., 2H, NH_2), 5.94 (s, 1H, H Th), 6.00 (s with ^{29}Si sat., 1H, $^2J_{HSi}$ = 11.0 Hz, H vinyl), 6.45 (d, 2H, $^3J_{HH}$ = 8.5 Hz, H Ph), 6.63 (s, 1H, H Th), 6.80 (d, 2H, $^3J_{HH}$ = 8.5 Hz, H Ph); ^{13}C{^{1}H} NMR (CD_2Cl_2, 100 MHz): δ (ppm) 14.5 (s, CH_3−Th), 14.6 (s, CH_3−Th), 15.2 (s, CH_3−Th), 15.4 (s, CH_3−Th), 19.9 (s, C *t*Bu), 20.1 (s, C *t*Bu), 29.1 (s, CH_3 *t*Bu), 29.3 (s, CH_3 *t*Bu), 114.0 (s, CH Ph), 126.5 (s, CH vinyl), 127.2 (s, CH Th), 128.0 (s, CH Th), 129.0 (s, CH Ph), 130.0 (s br., C Th), 132.6 (s, C Ph), 133.1 (s, C Th), 134.1 (s br., C Th), 135.1 (s, C Th), 137.3 (s, C Th), 138.1 (s, C Th), 140.2 (s, C−Si), 146.0 (s, C Ph), 151.3 (s, Si−CH=C−Ph), 163.1 (s, Si−C=C−Th); ^{29}Si NMR (CD_2Cl_2, 79 MHz): δ (ppm) 16.8 (s). HRMS (ESI, CH_3OH/CH_2Cl_2 (95/5)): calcd for $[C_{30}H_{39}NSiS_2+H]^+$, 506.2366; found, 506.2365 (0 ppm). Anal. Calcd for $[C_{30}H_{39}SiNS_2]$; C, 71.23; H, 7.77, N, 2.77. Found: C, 70.91; H, 7.62, N, 2.27.

Compound ***4f*** *(R = $N(CH_3)_2$).* After flash chromatography on silica gel [SiO_2, 15 g; eluent, DCM/pentane (50/50); R_f = 0.9], the product was obtained as a yellowish oil.

^{1}H NMR (CD_2Cl_2, 400 MHz): δ (ppm) 1.09 (s, 9H, CH_3 *t*Bu), 1.15 (s, 9H, CH_3 *t*Bu), 1.73 (s, 3H, CH_3−Th), 1.78 (s, 3H, CH_3−Th), 2.18 (s, 3H, CH_3−Th), 2.39 (s, 3H, CH_3−Th), 3.75 (s, 6H, N(CH_3)$_2$), 5.92 (s, 1H, H Th), 6.06 (s with ^{29}Si sat., 1H, $^2J_{HSi}$ = 11.0 Hz, H vinyl), 6.64 (s, 1H, H Th), 6.67 (d, 2H, $^3J_{HH}$ = 8.8 Hz, H Ph), 6.94 (d, 2H, $^3J_{HH}$ = 8.8 Hz, H Ph); ^{13}C{^{1}H} NMR (CD_2Cl_2, 100 MHz): δ (ppm) 14.5 (s, CH_3−Th), 14.6 (s, CH_3−Th), 15.1 (s, CH_3−Th), 15.4 (s, CH_3−Th), 19.9 (s, C *t*Bu), 20.1 (s, C *t*Bu), 29.0 (s, CH_3 *t*Bu), 29.3 (s, CH_3 *t*Bu), 55.5 (s, N(CH_3)$_2$), 112.9 (s, CH Ph), 127.1 (s, CH Th), 127.8 (s, CH vinyl), 127.9 (s, CH Th), 129.1 (s, CH Ph), 130.1 (s, C Th), 133.2 (s, C Th), 134.3 (s, C Th), 134.9 (s, C Ph), 135.2 (s, C Th), 137.1 (s, C Th), 138.0 (s, C Th), 140.3 (s, C−Si), 151.0 (s, Si−CH = C−Ph), 159.0 (s, C Ph), 162.8 (s, Si−C=C−Th); ^{29}Si NMR (CD_2Cl_2, 79 MHz): δ (ppm) 16.9 (s). HRMS (ESI, CH_3OH/CH_2Cl_2 (5/95)): calcd for $[C_{32}H_{43}SiNS_2+H]^+$, 534.2679; found, 534.2679 (0 ppm).

Compound ***5-D.*** The synthesis and purification of **5-D** were transposed from the described procedure for the protio-derivative **5** with Ph−C≡C−D as a starting material instead of Ph−C≡C−H.[17]

^{1}H NMR (CD_2Cl_2, 400 MHz): δ (ppm) 1.10 (s, 9H, CH_3-*t*Bu), 1.16 (s, 9H, CH_3-*t*Bu), 1.73 (s, 3H, CH_3−Th), 1.78 (s, 3H, CH_3−Th), 2.16 (s, 3H, CH_3−Th), 2.39 (s, 3H, CH_3−Th), 5.90 (s, 1H, H−Th), 6.65 (s, 1H, H−Th), 6.99−7.05 (m, 2H, H-*m*Ph), 7.11−7.19 (m, 3H, H-*o*Ph and H-*p*Ph); ^{13}C{^{1}H} NMR (CD_2Cl_2, 100 MHz): δ (ppm) 14.5 (s, CH_3−Th), 14.6 (s, CH_3−Th), 15.1 (s, CH_3−Th), 15.4 (s, CH_3−Th), 19.9 (s, C-*t*Bu), 20.1 (s, C-*t*Bu), 29.0 (s, CH_3-*t*Bu), 29.3 (s, CH_3-*t*Bu), 127.0 (s, CH-*p*Ph), 127.1 (s, CH−Th), 127.6 (s, CH-*o*Ph), 127.9 (s, CH−Th), 127.9 (s, CH-*m*Ph), 128.9 (triplet 111, $^1J_{CD}$ = 22.6 Hz, CD-vinyl), 130.1 (s, C2−Th), 133.3 (s, C2−Th), 134.4 (s, C5−Th), 135.3 (s, C5−Th), 137.0 (s, C3−Th), 137.9 (s, C3−Th), 140.3 (s, C−Si), 142.3 (s, C-*ipso*Ph), 150.8 (s, Si−C=C−Th), 163.3 (s, Si−CH=C-Ph). HRMS (ASAP, 90 °C): exact mass (monoisotopic) calcd for $[C_{30}H_{37}DSiS_2]^+$, 491.22415; found, 491.2246 (1 ppm).

Compound ***6-PtBu$_3$.*** A solution of silirene **1** (20.0 mg, 5.15×10^{-2} mmol) and bis(tri-*tert*-butylphosphine)palladium(0) (26.2 mg, 5.15×10^{-2} mmol, 1.00 equiv) in C_6D_6 (0.65 mL) was heated for 13 h at 50 °C, giving yellow solution. **6-PtBu$_3$** was characterized in situ by multinuclear NMR spectroscopy, showing a conversion toward the OA product of 40%.

^{1}H NMR (C_6D_6, 400 MHz): δ (ppm) 1.26 (d, 27H, $^3J_{HP}$ = 11.7 Hz, CH_3 P*t*Bu), 1.53 (s, 18H, CH_3 Si*t*Bu), 2.14 (s, 3H, CH_3−Th), 2.17 (s, 3H, CH_3−Th), 2.19 (s, 3H, CH_3−Th), 2.29 (s, 3H, CH_3−Th), 6.55 (s, 1H, H Th), 6.94 (s, 1H, H Th); ^{13}C{^{1}H} NMR (C_6D_6, 100 MHz): δ (ppm) 14.5 (s, CH_3−Th), 15.0 (s, CH_3−Th), 15.3 (s, CH_3−Th), 15.4 (s, CH_3−Th), 24.5 (s, C Si*t*Bu), 31.8 (s, CH_3 Si*t*Bu), 32.8 (d, $^2J_{CP}$ = 8.3 Hz, CH_3 P*t*Bu), 37.3 (s, C P*t*Bu), 127.3 (s, CH Th), 127.7 (s, CH Th), 128.4 (s, Cquat.), 128.9 (s, Cquat.), 134.3 (s, Cquat.), 134.6 (s, Cquat.),134.8 (d, J_{CP} = 2.4 Hz, Cquat.), 138.7 (d, J_{CP} = 8.8 Hz, Cquat.), 146.4 (d, J_{CP} = 12.8 Hz, Si−C=C), 151.5 (d, J_{CP} = 46.1 Hz, Si−C=C); ^{29}Si{^{1}H} NMR (C_6D_6, 79 MHz): δ (ppm) −33.7 (s); ^{31}P{^{1}H} NMR (C_6D_6, 202 MHz): δ (ppm) 80.9 (s).

Compound ***6-P(otol)$_3$.*** A solution of silirene **1** (20.0 mg, 5.15×10^{-2} mmol) and bis(tri-*o*-tolyl-phosphine)palladium(0) (36.8 mg, 5.15×10^{-2} mmol, 1.00 equiv) in C_6D_6 (0.65 mL) was heated for 4 h at 50 °C, giving yellow solution. **6-P(*o*tol)$_3$** was characterized in situ by multinuclear NMR spectroscopy, showing a conversion toward the OA product of 82%.

^{1}H NMR (C_6D_6, 400 MHz): δ (ppm) 1.35 (s, 18H, CH_3 Si*t*Bu), 1.97 (s, 3H, CH_3−Th), 2.15 (s, 3H, CH_3−Th), 2.18 (s, 3H, CH_3−Th), 2.25 (s, 3H, CH_3−Th), 2.46 (s, 3H, CH_3 tolyl), 6.56 (s, 1H, H Th), 6.96 (s, 1H, H Th); the ortho tolyl proton resonance signals could not be unambiguously assigned due to the complexity of the aromatic region of the spectrum; ^{13}C{^{1}H} NMR (C_6D_6, 100 MHz): δ (ppm) 14.7 (s, CH_3−Th), 15.1 (s, CH_3−Th), 15.1 (s, CH_3−Th), 15.3 (s, CH_3−Th), 23.7 (d, $^3J_{CP}$ = 11.8 Hz, CH_3 tolyl), 24.7 (s, C Si*t*Bu), 31.3 (s, CH_3 Si*t*Bu), 126.0 (d, J_{CP} = 8.9 Hz, CH tolyl), 127.0 (s, CH Th), 127.5 (s, CH Th), 128.5 (s br., Cquat.), 129.3 (s, Cquat.), 130.0 (d, $^1J_{CP}$ = 28.7 Hz, P−C), 130.4 (s br., CH tolyl), 131.9 (d, $^3J_{CP}$ = 5.8 Hz, CH tolyl), 134.8 (s, Cquat.), 134.9 (s, Cquat.), 135.5 (d, J_{CP} = 14.7 Hz, CH tolyl), 137.8 (d, J_{CP} = 1.2 Hz, Cquat.), 138.7 (d, J_{CP} = 9.3 Hz, Cquat.), 142.9 (d, J_{CP} = 11.6 Hz, C *o*tolyl), 146.0 (d, J_{CP} =

https://doi.org/10.1021/acs.inorgchem.3c00045
Inorg. Chem. XXXX, XXX, XXX−XXX

11.7 Hz, Si−C=C), 152.6 (d, J_{CP} = 55.0 Hz, Si−C=C); $^{29}Si\{^1H\}$ NMR (C_6D_6, 79 MHz): δ (ppm) −31.6 (s); $^{31}P\{^1H\}$ NMR (C_6D_6, 162 MHz): δ (ppm) 25.3 (s).

Compound 6-COD. THF (2 mL) was added to a neat mixture of silirene **1** (30.0 mg, 7.72 × 10^{-2} mmol) and (1,5-cyclooctadiene)-bis(trimethylsilylmethyl)palladium(II) (30.0 mg, 7.72 × 10^{-2} mmol, 1.00 equiv), and the resulting solution was stirred for 1 h at room temperature, giving a dark solution. The solvent was evaporated under vacuum, and the residue thus obtained was further dried for 10 h under vacuum, giving a sticky brown residue. The residue was extracted with pentane (2 mL), and the pentane solution was filtered and placed at −30 °C, giving the expected compound as colorless blocks in 41% yield. Single crystals suitable for X-ray diffraction analysis were obtained in the same conditions.

^1H NMR (CD_2Cl_2, 500 MHz, 243 K): δ (ppm) 1.07 (s, 18H, C$\underline{H}_3$ Si*t*Bu), 1.96 (s, 3H, C$\underline{H}_3$−Th), 1.98 (s, 3H, C$\underline{H}_3$−Th), 2.06−2.20 (br., 2H, C$\underline{H}_2$ COD), 2.20−2.40 (br., 4H, C$\underline{H}_2$ COD), 2.29 (s, 3H, C$\underline{H}_3$−Th), 2.30 (s, 3H, C$\underline{H}_3$−Th), 2.52−2.66 (br., 2H, C$\underline{H}_2$ COD), 4.88−5.67 (br., 2H, C$\underline{H}$ COD), 5.90 (br., 2H, C$\underline{H}$ COD), 6.27 (s, 1H, $\underline{H}$ Th), 6.43 (s, 1H, $\underline{H}$ Th); $^{13}C\{^1H\}$ NMR (CD_2Cl_2, 125 MHz, 243 K): δ (ppm) 14.0 (s, $\underline{C}H_3$−Th), 14.7 (s, $\underline{C}H_3$−Th), 15.2 (s, $\underline{C}H_3$−Th), 15.2 (s, $\underline{C}H_3$−Th), 23.3 (s br., $\underline{C}$ Si*t*Bu), 27.4 (br., $\underline{C}H_2$ COD), 30.0 (br., $\underline{C}H_2$ COD), 30.7 (s, $\underline{C}H_3$ Si*t*Bu), 105.1 (s. br., $\underline{C}$H COD), 122.2 (s. br., $\underline{C}$H COD), 123.2 (s, $\underline{C}$quat.), 125.4 (s, $\underline{C}$H Th), 126.4 (s, $\underline{C}$quat.), 126.5 (s, $\underline{C}$H Th), 133.8, 133.8, 140.8, 146.4, 151.6 and 161.3 (s, $\underline{C}$quat.); $^{29}Si\{^1H\}$ NMR (CD_2Cl_2, 99 MHz, 243 K): δ (ppm) −34.8 (s).

Compound 6-PPh$_3$. To a solution of silirene **1** (40.0 mg, 0.103 mmol) and triphenylphosphine (27.0 mg, 0.103 mmol, 1.00 equiv) in THF (2.5 mL) was added (1,5-cyclooctadiene)bis-(trimethylsilylmethyl)palladium(II) (40.1 mg, 0.103 mmol, 1.00 equiv) as a powder in one portion, and the resulting mixture was stirred for 1 h at room temperature, giving a clear green solution.

The volatiles were then eliminated under reduced pressure, and the residue was then dried under vacuum (2 × 10^{-2} mmbar) for 10 h, giving a green solid. This solid was then washed two times with pentane (2 times 1 mL), giving the expected compound as a clear yellow powder in 65% yield (51 mg). All the attempts to grow single crystals of **6-PPh$_3$** for X-ray diffraction analysis furnished crystals of the known complex [Pd(PPh$_3$)$_3$].

^1H NMR (THF-d^8, 400 MHz): δ (ppm) 1.04 (s, 18H, C$\underline{H}_3$ *t*Bu), 1.86 (s, 3H, C$\underline{H}_3$−Th), 2.13 (s, 3H, C$\underline{H}_3$−Th), 2.32 (s, 3H, C$\underline{H}_3$−Th), 2.34 (s, 3H, C$\underline{H}_3$−Th), 6.56 (s, 1H, $\underline{H}$ Th), 6.58 (s, 1H, $\underline{H}$ Th), 7.31−7.43 (m, 9H, $\underline{H}$ *p*Ph and $\underline{H}$ *m*Ph), 7.54−7.64 (m, 6H, $\underline{H}$ *o*Ph); $^{13}C\{^1H\}$ NMR (THF-d^8, 100 MHz): δ (ppm) 14.7 (s, $\underline{C}H_3$−Th), 14.9 (s, $\underline{C}H_3$−Th), 15.0 (s, $\underline{C}H_3$−Th), 15.1 (s, $\underline{C}H_3$−Th), 24.7 (s, $\underline{C}$ *t*Bu), 31.1 (s, $\underline{C}H_3$ *t*Bu), 127.3 (s, $\underline{C}$H Th), 127.6 (s, $\underline{C}$H Th), 128.7 (d, J_{CP} = 1.7 Hz, $\underline{C}$quat.), 129.2 (s, $\underline{C}$quat.), 129.2 (d, J_{CP} = 9.6 Hz, $\underline{C}$H *m*Ph), 130.6 (d, J_{CP} = 1.4 Hz, $\underline{C}$H *p*Ph), 134.7 (s, $\underline{C}$quat.), 135.0 (d, J_{CP} = 15.9 Hz, $\underline{C}$H *o*Ph), 135.3 (d, $^1J_{CP}$ = 31.2 Hz, $\underline{C}$−P), 135.4 (s, $\underline{C}$quat.), 137.0 (s br., $\underline{C}$quat.), 138.9 (d, J_{CP} = 9.9 Hz, $\underline{C}$quat.), 146.3 (d, J_{CP} = 11.5 Hz, Si−$\underline{C}$=C), 156.0 (d, J_{CP} = 63.4 Hz, Si−C=$\underline{C}$); $^{29}Si\{^1H\}$ NMR (THF-d^8, 79 MHz): δ (ppm) −27.2 (d, J_{SiP} = 2.1 Hz); $^{31}P\{^1H\}$ NMR (THF-d^8, 162 MHz): δ (ppm) 24.0 (s, **6-PPh$_3$**).

NMR Evidence for the Existence of an Equilibrium. In the NOESY $^1H,^1H$ NMR spectrum, exchange correlations are observed between PPh$_3$ aromatic proton resonance signals of **6-PPh$_3$** and [Pd(PPh$_3$)$_n$]; exchange correlations are observed between thienyl −CH$_3$ protons resonance signals of **6-PPh$_3$** and **6-PPh$_3$**.

In the NOESY $^{31}P,^{31}P$ NMR spectrum, exchange correlations are observed between the PPh$_3$ resonance signal of **6-PPh$_3$** and [Pd(PPh$_3$)$_n$].

Compound 6-P(OPh)$_3$. To a solution of silirene **1** (100 mg, 0.257 mmol) and triphenylphosphite (67.4 μL, 79.8 mg, 0.257 mmol, 1.00 equiv) in THF (7 mL) was added (1,5-cyclooctadiene)bis-(trimethylsilylmethyl)palladium(II) (100 mg, 0.257 mmol, 1.00 equiv) as a powder in one portion, and the resulting mixture was stirred for 2 h at room temperature, giving a clear yellow solution.

The crude mixture was then filtered, and the resulting solution was concentrated to dryness over 30 min at room temperature. The resulting residue was extracted with pentane (15 mL) at room temperature and filtered, and the yellow pentane solution was placed in the freezer at −40 °C, affording colorless crystals in a few hours. The mother liquor was then eliminated via a syringe, and the crystals were washed 4 times with −40 °C cold pentane (4 times 5 mL). The crystals were then dried under vacuum at 0 °C for 5 h. NMR analysis of the crystalline material revealed the presence of about 5% of [Pd(P(OPh)$_3$)$_3$] in addition to the expected compound (46% yield). Attempts to separate the two complexes were unsuccessful. Crystals of **6-P(OPh)$_3$** suitable for X-ray diffraction were obtained from a saturated THF/pentane solution at −30 °C.

The compound **6-P(OPh)$_3$** was characterized by NMR at −40 °C in THF ^{8}d. In the case of ^{29}Si NMR, no resonance signal could be observed at low temperature, and the spectrum was recorded at room temperature over a few hours, resulting in the partial decomposition of the compound due to its thermal instability. Fast ^1H and ^{31}P NMR spectra could also be recorded at room temperature in CD_2Cl_2 for a better resolution (see S101−104).

^1H NMR (THF-d^8, 400 MHz, 233 K): δ (ppm) 1.30 (s, 18H, C$\underline{H}_3$ *t*Bu), 1.68 (s, 3H, C$\underline{H}_3$−Th), 1.75 (s, 3H, C$\underline{H}_3$−Th), 2.19 (s, 3H, C$\underline{H}_3$−Th), 2.34 (s, 3H, C$\underline{H}_3$−Th), 6.08 (s, 1H, $\underline{H}$ Th), 6.55 (s, 1H, $\underline{H}$ Th), 7.17−7.24 (m, 3H, $\underline{H}$ *p*Ph), 7.35−7.45 (m, 12H, $\underline{H}$ *o*Ph and $\underline{H}$ *m*Ph); $^{13}C\{^1H\}$ NMR (THF-d^8, 100 MHz, 233 K): δ (ppm) 14.4 (s, $\underline{C}H_3$−Th), 14.7 (s, $\underline{C}H_3$−Th), 14.9 (s, $\underline{C}H_3$−Th), 15.3 (s, $\underline{C}H_3$−Th), 24.2 (s, $\underline{C}$ *t*Bu), 31.2 (s, $\underline{C}H_3$ *t*Bu), 121.8 (br., $\underline{C}$H *o*Ph or $\underline{C}$H *m*Ph), 125.4 (s, $\underline{C}$H *m*Ph), 126.1 (br., $\underline{C}$quat.), 127.1 (s, $\underline{C}$H Th), 127.8 (s, $\underline{C}$H Th or $\underline{C}$quat.), 127.9 (s, $\underline{C}$H Th or $\underline{C}$quat.), 130.3 (s, $\underline{C}$H *o*Ph or $\underline{C}$H *m*Ph), 133.4 (br., $\underline{C}$quat.), 134.5 (s, $\underline{C}$quat.), 141.0 (d br., J_{CP} = 12.3 Hz, $\underline{C}$quat.), 143.4 (br., $\underline{C}$quat.), 151.8 (d, $^1J_{CP}$ = 3.5 Hz, $\underline{C}$−P), 165.3 (d, $^1J_{CP}$ = 151.7 Hz, $\underline{C}$quat.); $^{29}Si\{^1H\}$ NMR (C_6D_6, 79 MHz, 293 K): δ (ppm) −26.9 (d, J_{SiP} = 4.7 Hz); $^{31}P\{^1H\}$ NMR (THF-d^8, 162 MHz, 233 K): δ (ppm) 126.8 (s). One quaternary carbon was not observed.

■ ASSOCIATED CONTENT

Supporting Information

The Supporting Information is available free of charge at https://pubs.acs.org/doi/10.1021/acs.inorgchem.3c00045.

Experimental details and characterization data and Cartesian coordinates for the calculated structure obtained by DFT calculations (PDF).

Accession Codes

CCDC 2184696−2184699 contain the supplementary crystallographic data for this paper. These data can be obtained free of charge via www.ccdc.cam.ac.uk/data_request/cif, or by emailing data_request@ccdc.cam.ac.uk, or by contacting The Cambridge Crystallographic Data Centre, 12 Union Road, Cambridge CB2 1EZ, UK; fax: +44 1223 336033.

■ AUTHOR INFORMATION

Corresponding Authors

Marc Devillard − *ISCR (Institut des Sciences Chimiques de Rennes)—UMR 6226, Université de Rennes 1, CNRS, F-35042 Rennes, France;* orcid.org/0000-0002-3821-0885; Email: marc.devillard@univ-rennes1.fr

Gilles Alcaraz − *ISCR (Institut des Sciences Chimiques de Rennes)—UMR 6226, Université de Rennes 1, CNRS, F-35042 Rennes, France;* orcid.org/0000-0001-8705-5917; Email: gilles.alcaraz@univ-rennes1.fr

Authors

Chiara Dinoi − *LCPNO, CNRS & INSA, Université de Toulouse, F-31077 Toulouse, France*

Iker Del Rosal − *LCPNO, CNRS & INSA, Université de Toulouse, F-31077 Toulouse, France;* orcid.org/0000-0001-6898-4550

https://doi.org/10.1021/acs.inorgchem.3c00045
Inorg. Chem. XXXX, XXX, XXX−XXX

Clément Orione − *ScanMAT-CRMPO, Université de Rennes 1, F-35042 Rennes, France*
Marie Cordier − *ISCR (Institut des Sciences Chimiques de Rennes)—UMR 6226, Université de Rennes 1, CNRS, F-35042 Rennes, France*

Complete contact information is available at:
https://pubs.acs.org/10.1021/acs.inorgchem.3c00045

Notes

The authors declare no competing financial interest.

■ ACKNOWLEDGMENTS

We thank Dr. P. Jéhan (CRMPO, Rennes) and F. Lambert (CRMPO, Rennes) for the HRMS analyses, M. Escadeillas (CRMPO, Rennes) for the elemental analyses, and E. Caytan (ISCR, Rennes) for NMR analyses. This work was performed using HPC resources from CALMIP (Grant 2017-[p17010]). We also thank the CINES for the computing resources (Montpellier, allocation 2019-A0060810728 and 2020-AP010811752 awarded by GENCI).

■ REFERENCES

(1) Planells, A. R.; Ferao, A. E. Accurate Ring Strain Energy Calculations on Saturated Three-Membered Heterocycles with One Group 13−16 Element. *Inorg. Chem.* **2020**, *59*, 11503−11513.

(2) (a) Romero, A. H. Influence of the heteroatom on the structure, bonding and ring strain of a series of three-membered rings containing a second, third, fourth and fifth row elements: a theoretical investigation. *Struct. Chem.* **2018**, *29*, 1623−1636. (b) Aysin, R. R.; Leites, L. A.; Bukalov, S. S. Aromaticity of 1-Heterocyclopropenes Containing an Atom of Group 14 or 4. *Organometallics* **2020**, *39*, 2749−2762. (c) Göller, A.; Clark, T. σ^*-Aromaticity in Three-Membered Rings. *J. Mol. Model.* **2000**, *6*, 133−149. (d) Méndez-Rojas, M. A.; Merino, G. 1.09 - Three-membered Rings with One Silicon, Germanium, Tin or Lead Atom. In *Comprehensive Heterocyclic Chemistry III*; Katritzky, A. R., Ramsden, C. A., Scriven, E. F. V., Taylor, R. J. K., Eds.; Elsevier, 2008; pp 483−512.

(3) Huang, C.-Y.; Doyle, A. G. The Chemistry of Transition Metals with Three-Membered Ring Heterocycles. *Chem. Rev.* **2014**, *114*, 8153−8198.

(4) (a) Mathey, F.; Regitz, M. 2.1 - Three-membered Rings: 1. Phosphiranes and Phosphirenes. In *Phosphorus-Carbon Heterocyclic Chemistry*; Mathey, F., Ed.; Elsevier Science Ltd, 2001; pp 17−55. (b) Delouche, T.; Taifour, G.; Cordier, M.; Roisnel, T.; Tondelier, D.; Manzhi, P.; Geffroy, B.; Le Guennic, B.; Jacquemin, D.; Hissler, M.; et al. Si-containing polycyclic aromatic hydrocarbons: synthesis and opto-electronic properties. *Chem. Commun.* **2022**, *58*, 88−91.

(5) (a) Franz, A. K.; Woerpel, K. A. Development of Reactions of Silacyclopropanes as New Methods for Stereoselective Organic Synthesis. *Acc. Chem. Res.* **2000**, *33*, 813−820. (b) Nandi, G. C. Advances in the Synthesis and Applications of Three Membered Sila, Sila-Aza/-Phospha/-Oxa/-Thia Cyclopropanes. *Eur. J. Org. Chem.* **2020**, *2021*, 587−606. (c) Anderson, L. L.; Woerpel, K. A. Formation and Utility of Azasilacyclopentadienes Derived from Silacyclopropenes and Nitriles. *Org. Lett.* **2009**, *11*, 425−428. (d) Greene, M. A.; Prévost, M.; Tolopilo, J.; Woerpel, K. A. Diastereoselective Synthesis of Seven-Membered-Ring trans-Alkenes from Dienes and Aldehydes by Silylene Transfer. *J. Am. Chem. Soc.* **2012**, *134*, 12482−12484. (e) Rotsides, C. Z.; Woerpel, K. A. Insertion Reactions of Silacyclopropanes: Evidence for a Radical-Based Mechanism. *Organometallics* **2016**, *35*, 3132−3138. (f) Nobis, M.; Inoue, S.; Rieger, B. Modular silacyclopropenes: synthesis and application for Si−H containing substrate functionalization. *Chem. Commun.* **2022**, *58*, 11159−11162. (g) Nobis, M.; Futter, J.; Moxter, M.; Inoue, S.; Rieger, B. Photo-Activity of Silacyclopropenes and their Application in Metal-Free Curing of Silicones. *ChemSusChem* **2023**, *16*, No. e202201957.

(6) (a) Mu, Q.-C.; Chen, J.; Xia, C.-G.; Xu, L.-W. Synthesis of silacyclobutanes and their catalytic transformations enabled by transition-metal complexes. *Coord. Chem. Rev.* **2018**, *374*, 93−113. (b) Mohseni-Ala, J.; Auner, N. Silacyclobutenes − Synthesis and reactivity. *Inorg. Chim. Acta* **2006**, *359*, 4677−4697. (c) Ishikawa, M.; Naka, A.; Kobayashi, H. The chemistry of silacyclobutenes: Synthesis, reactions, and theoretical studies. *Coord. Chem. Rev.* **2017**, *335*, 58−75. (d) Qin, Y.; Han, J. L.; Ju, C. W.; Zhao, D. Ring Expansion to 6-7- and 8-Membered Benzosilacycles through Strain-Release Silicon-Based Cross-Coupling. *Angew. Chem., Int. Ed.* **2020**, *59*, 8481−8485. (e) Zhu, M.-H.; Zhang, X.-W.; Usman, M.; Cong, H.; Liu, W.-B. Palladium-Catalyzed (4 + 4) Annulation of Silacyclobutanes and 2-Iodobiarenes to Eight-Membered Silacycles via C−H and C−Si Bond Activation. *ACS Catal.* **2021**, *11*, 5703−5708. (f) Wang, X. C.; Wang, H. R.; Xu, X.; Zhao, D. Ring Expansion to 8-Membered Silacycles through Formal Cross-Dimerization of 5-Membered Palladacycles with Silacyclobutanes. *Eur. J. Org. Chem.* **2021**, *2021*, 3039−3042. (g) Shintani, R.; Moriya, K.; Hayashi, T. Palladium-Catalyzed Desymmetrization of Silacyclobutanes with Alkynes: Enantioselective Synthesis of Silicon-Stereogenic 1-Sila-2-cyclohexenes and Mechanistic Considerations. *Org. Lett.* **2012**, *14*, 2902−2905. (h) Chen, H.; Chen, Y.; Tang, X.; Liu, S.; Wang, R.; Hu, T.; Gao, L.; Song, Z. Rhodium-Catalyzed Reaction of Silacyclobutanes with Unactivated Alkynes to Afford Silacyclohexenes. *Angew. Chem., Int. Ed.* **2019**, *58*, 4695−4699. (i) Huo, J.; Zhong, K.; Xue, Y.; Lyu, M.; Ping, Y.; Liu, Z.; Lan, Y.; Wang, J. Palladium-Catalyzed Enantioselective Carbene Insertion into Carbon−Silicon Bonds of Silacyclobutanes. *J. Am. Chem. Soc.* **2021**, *143*, 12968−12973.

(7) (a) Hermanns, J.; Schmidt, B. Five- and six-membered silicon−carbon heterocycles. Part 1. Synthetic methods for the construction of silacycles. *J. Chem. Soc., Perkin Trans. 1* **1998**, *1*, 2209−2230. (b) Huo, J.; Zhong, K.; Xue, Y.; Lyu, M.; Ping, Y.; Ouyang, W.; Liu, Z.; Lan, Y.; Wang, J. Ligand-Controlled Site- and Enantioselective Carbene Insertion into Carbon-Silicon Bonds of Benzosilacyclobutanes. *Chemistry* **2022**, *28*, No. e202200191.

(8) (a) Sanzone, J. R.; Woerpel, K. A. High Reactivity of Strained Seven-Membered-Ring trans-Alkenes. *Angew. Chem., Int. Ed.* **2016**, *55*, 790−793. (b) Sanzone, J. R.; Hu, C. T.; Woerpel, K. A. Uncatalyzed Carboboration of Seven-Membered-Ring trans-Alkenes: Formation of Air-Stable Trialkylboranes. *J. Am. Chem. Soc.* **2017**, *139*, 8404−8407. (c) Greene, M. A.; Liu, Y.; Sanzone, J. R.; Woerpel, K. A. Carboalumination of Seven-Membered-Ring trans-Alkenes. *Org. Lett.* **2020**, *22*, 7518−7521.

(9) (a) Tamao, K.; Uchida, M.; Izumizawa, T.; Furukawa, K.; Yamaguchi, S. Silole Derivatives as Efficient Electron Transporting Materials. *J. Am. Chem. Soc.* **1996**, *118*, 11974−11975. (b) Yamaguchi, S.; Tamao, K. Theoretical Study of the Electronic Structure of 2,2′-Bisilole in Comparison with 1,1′-Bi-1,3-cyclopentadiene: σ^*−π^* Conjugation and a Low-Lying LUMO as the Origin of the Unusual Optical Properties of 3,3′,4,4′-Tetraphenyl-2,2′-bisilole. *Bull. Chem. Soc. Jpn.* **1996**, *69*, 2327−2334. (c) Yamaguchi, S.; Tamao, K. Silole-containing σ- and π-conjugated compounds. *J. Chem. Soc., Dalton Trans.* **1998**, 3693−3702. (d) Hissler, M.; Dyer, P. W.; Réau, R. Linear organic π-conjugated systems featuring the heavy Group 14 and 15 elements. *Coord. Chem. Rev.* **2003**, *244*, 1−44. (e) Zhan, X.; Barlow, S.; Marder, S. R. Substituent effects on the electronic structure of siloles. *Chem. Commun.* **2009**, *15*, 1948−1955.

(10) (a) Corey, J. Y. Siloles Part 1: Synthesis, Characterization, and Applications. *Adv. Organomet. Chem.* **2011**, *59*, 1−180. (b) Santra, S. Synthesis and Application of Siloles: From the Past to Present. *ChemistrySelect* **2020**, *5*, 9034−9058.

(11) (a) Furukawa, S.; Kobayashi, J.; Kawashima, T. Development of a Sila-Friedel−Crafts Reaction and Its Application to the Synthesis of Dibenzosilole Derivatives. *J. Am. Chem. Soc.* **2009**, *131*, 14192−14193. (b) Furukawa, S.; Kobayashi, J.; Kawashima, T. Application of the sila-Friedel−Crafts reaction to the synthesis of π-extended silole derivatives and their properties. *Dalton Trans.* **2010**, *39*, 9329−9336.

(c) Dong, Y.; Takata, Y.; Yoshigoe, Y.; Sekine, K.; Kuninobu, Y. Lewis acid-catalyzed synthesis of silafluorene derivatives from biphenyls and dihydrosilanes via a double sila-Friedel−Crafts reaction. *Chem. Commun.* **2019**, *55*, 13303−13306.

(12) (a) Liang, Y.; Zhang, S.; Xi, Z. Palladium-Catalyzed Synthesis of Benzosilolo[2,3-b]indoles via Cleavage of a C(sp3)−Si Bond and Consequent Intramolecular C(sp2)−Si Coupling. *J. Am. Chem. Soc.* **2011**, *133*, 9204−9207. (b) Kuninobu, Y.; Yamauchi, K.; Tamura, N.; Seiki, T.; Takai, K. Rhodium-catalyzed asymmetric synthesis of spirosilabifluorene derivatives. *Angew. Chem., Int. Ed.* **2013**, *52*, 1520−1522. (c) Murai, M.; Matsumoto, K.; Takeuchi, Y.; Takai, K. Rhodium-Catalyzed Synthesis of Benzosilolometallocenes via the Dehydrogenative Silylation of C(sp2)−H Bonds. *Org. Lett.* **2015**, *17*, 3102−3105. (d) Shibata, T.; Shizuno, T.; Sasaki, T. Enantioselective synthesis of planar-chiral benzosiloloferrocenes by Rh-catalyzed intramolecular C−H silylation. *Chem. Commun.* **2015**, *51*, 7802−7804. (e) Zhang, Q. W.; An, K.; Liu, L. C.; Yue, Y.; He, W. Rhodium-catalyzed enantioselective intramolecular C-H silylation for the syntheses of planar-chiral metallocene siloles. *Angew. Chem., Int. Ed.* **2015**, *54*, 6918−6921. (f) Zhang, Q. W.; An, K.; Liu, L. C.; Zhang, Q.; Guo, H.; He, W. Construction of Chiral Tetraorganosilicons by Tandem Desymmetrization of Silacyclobutanes/Intermolecular Dehydrogenative Silylation. *Angew. Chem., Int. Ed.* **2017**, *56*, 1125−1129. (g) Zhang, L.; An, K.; Wang, Y.; Wu, Y.-D.; Zhang, X.; Yu, Z.-X.; He, W. A Combined Computational and Experimental Study of Rh-Catalyzed C−H Silylation with Silacyclobutanes: Insights Leading to a More Efficient Catalyst System. *J. Am. Chem. Soc.* **2021**, *143*, 3571−3582. (h) Shintani, R.; Kurata, H.; Nozaki, K. Rhodium-catalyzed intramolecular alkynylsilylation of alkynes. *Chem. Commun.* **2015**, *51*, 11378−11381. (i) Chen, S.; Mu, D.; Mai, P.-L.; Ke, J.; Li, Y.; He, C. Enantioselective construction of six- and seven-membered triorgano-substituted silicon-stereogenic heterocycles. *Nat. Commun.* **2021**, *12*, 1249.

(13) (a) Matsuda, T.; Kadowaki, S.; Yamaguchi, Y.; Murakami, M. Gold-catalysed intramolecular trans-allylsilylation of alkynes forming 3-allyl-1-silaindenes. *Chem. Commun.* **2008**, *24*, 2744. (b) Shimizu, M.; Mochida, K.; Hiyama, T. Modular approach to silicon-bridged biaryls: palladium-catalyzed intramolecular coupling of 2-(arylsilyl)-aryl triflates. *Angew. Chem., Int. Ed.* **2008**, *47*, 9760−9764. (c) Mochida, K.; Shimizu, M.; Hiyama, T. Palladium-Catalyzed Intramolecular Coupling of 2-[(2-Pyrrolyl)silyl]aryl Triflates through 1,2-Silicon Migration. *J. Am. Chem. Soc.* **2009**, *131*, 8350−8351. (d) Shintani, R.; Otomo, H.; Ota, K.; Hayashi, T. Palladium-Catalyzed Asymmetric Synthesis of Silicon-Stereogenic Dibenzosiloles via Enantioselective C−H Bond Functionalization. *J. Am. Chem. Soc.* **2012**, *134*, 7305−7308.

(14) (a) Matsuda, T.; Kadowaki, S.; Goya, T.; Murakami, M. Synthesis of Silafluorenes by Iridium-Catalyzed [2 + 2 + 2] Cycloaddition of Silicon-Bridged Diynes with Alkynes. *Org. Lett.* **2007**, *9*, 133. (b) Ohmura, T.; Masuda, K.; Suginome, M. Silylboranes Bearing Dialkylamino Groups on Silicon as Silylene Equivalents: Palladium-Catalyzed Regioselective Synthesis of 2,4-Disubstituted Siloles. *J. Am. Chem. Soc.* **2008**, *130*, 1526−1527. (c) Ohmura, T.; Masuda, K.; Takase, I.; Suginome, M. Palladium-Catalyzed Silylene-1,3-Diene [4 + 1] Cycloaddition with Use of (Aminosilyl)boronic Esters as Synthetic Equivalents of Silylene. *J. Am. Chem. Soc.* **2009**, *131*, 16624−16625. (d) Yabusaki, Y.; Ohshima, N.; Kondo, H.; Kusamoto, T.; Yamanoi, Y.; Nishihara, H. Versatile synthesis of blue luminescent siloles and germoles and hydrogen-bond-assisted color alteration. *Chem.—Eur. J.* **2010**, *16*, 5581−5585. (e) Tobisu, M.; Onoe, M.; Kita, Y.; Chatani, N. Rhodium-Catalyzed Coupling of 2-Silylphenylboronic Acids with Alkynes Leading to Benzosiloles: Catalytic Cleavage of the Carbon−Silicon Bond in Trialkylsilyl Groups. *J. Am. Chem. Soc.* **2009**, *131*, 7506−7507. (f) Onoe, M.; Baba, K.; Kim, Y.; Kita, Y.; Tobisu, M.; Chatani, N. Rhodium-Catalyzed Carbon−Silicon Bond Activation for Synthesis of Benzosilole Derivatives. *J. Am. Chem. Soc.* **2012**, *134*, 19477−19488. (g) Liang, Y.; Geng, W.; Wei, J.; Xi, Z. Palladium-Catalyzed Intermolecular Coupling of 2-Silylaryl Bromides with Alkynes: Synthesis of Benzosiloles and Heteroarene-Fused Siloles by Catalytic Cleavage of the C(sp3)-Si Bond. *Angew. Chem., Int. Ed.* **2012**, *51*, 1934−1937.

(15) (a) Seyferth, D.; Duncan, D. P.; Vick, S. C. Novel two atom insertions into the silacyclopropane and silacyclopropene rings. *J. Organomet. Chem.* **1977**, *125*, C5−C10. (b) Seyferth, D.; Vick, S. C.; Shannon, M. L.; Lim, T. F. O.; Duncan, D. P. Two atom insertions into the silacyclopropane and silacyclopropene rings: mechanistic considerations. *J. Organomet. Chem.* **1977**, *135*, C37−C44. (c) Boudjouk, P.; Samaraweera, U.; Sooriyakumaran, R.; Chrusciel, J.; Anderson, K. R. Convenient Routes to Di-tert-butylsilanediyl: Chemical, Thermal and Photochemical Generation. *Angew. Chem., Int. Ed.* **1988**, *27*, 1355−1356. (d) Belzner, J.; Ihmels, H. A novel route to stable silacyclopropenes - First synthesis of silacyclopropenes bearing vinylic hydrogen. *Tetrahedron Lett.* **1993**, *34*, 6541−6544.

(16) (a) Palmer, W. S.; Woerpel, K. A. Synthesis of Silirenes by Palladium-Catalyzed Transfer of Silylene from Siliranes to Alkynes. *Organometallics* **1997**, *16*, 4824−4827. (b) Palmer, W. S.; Woerpel, K. A. Palladium-Catalyzed Reactions of Di-tert-butylsiliranes with Electron-Deficient Alkynes and Investigations of the Catalytic Cycle. *Organometallics* **2001**, *20*, 3691−3697. (c) Buchner, K. M.; Woerpel, K. A. Palladium- and Nickel-Catalyzed Carbon−Carbon Bond Insertion Reactions with Alkylidenesilacyclopropanes. *Organometallics* **2010**, *29*, 1661−1669.

(17) Devillard, M.; Nour Eddine, N.; Cordier, M.; Alcaraz, G. Dithienylethene-Based Photochromic Siloles: A Straightforward and Divergent Synthetic Strategy. *Angew. Chem., Int. Ed.* **2021**, *60*, 12356−12359.

(18) Seyferth, D.; Shannon, M. L.; Vick, S. C.; Lim, T. F. O. Silacyclopropenes. 3. Palladium-catalyzed insertion reactions. *Organometallics* **1985**, *4*, 57−62.

(19) Ishikawa, M.; Naka, A.; Ohshita, J. The Chemistry of Silacyclopropenes. *Asian J. Org. Chem.* **2015**, *4*, 1192−1209.

(20) Herz, F. A. D.; Nobis, M.; Wendel, D.; Pahl, P.; Altmann, P. J.; Tillmann, J.; Weidner, R.; Inoue, S.; Rieger, B. Application of multifunctional silylenes and siliranes as universal crosslinkers for metal-free curing of silicones. *Green Chem.* **2020**, *22*, 4489−4497.

(21) (a) Ishikawa, M.; Fuchikami, T.; Kumada, M. [PdCl2(PEt3)2]-Catalysed formation of 1,4-disilacyclohexa-2,5-diene from 1-silacyclopropene. *J. Chem. Soc., Chem. Commun.* **1977**, *10*, 352a. (b) Ishikawa, M.; Sugisawa, H.; Kumada, M.; Higuchi, T.; Matsui, K.; Hirotsu, K. Palladium-catalyzed formation of 1,4-disila-2,5-cyclohexadienes from 1-silacyclopropenes. *Organometallics* **1982**, *1*, 1473−1477.

(22) The monitoring of the reaction includes the previously described ethynylbenzene [R = H (compound **5**)]. In the case of the amino substituents [R = NH_2 (**4e**) and NMe_2 (**4f**)], the results were not included due to the instantaneous coordination of the substrate to Pd(0) hampering a meaningful comparison with the other −R groups.

(23) (a) Ikenaga, K.; Hiramatsu, K.; Nasaka, N.; Matsumoto, S. (Trialkylstannyl)dimethylsilane as a new precursor of dimethylsilylene: a novel synthesis of 3,4-disubstituted 1-silacyclopenta-2,4-dienes. *J. Org. Chem.* **1993**, *58*, 5045−5047. (b) Li, L.; Zhang, Y.; Gao, L.; Song, Z. Recent advances in C−Si bond activation via a direct transition metal insertion. *Tetrahedron Lett.* **2015**, *56*, 1466−1473. (c) Tahara, A.; Nagino, S.; Sunada, Y.; Haige, R.; Nagashima, H. Syntheses of Substituted 1,4-Disila-2,5-cyclohexadienes from Cyclic Hexasilane Si6Me12 and Alkynes via Successive Si−Si Bond Activation by Pd/Isocyanide Catalysts. *Organometallics* **2018**, *37*, 2531−2543.

(24) (a) Ishikawa, M.; Sugisawa, H.; Harata, O.; Kumada, M. Nickel-catalyzed reaction of silacyclopropenes with acetylenes. in convenient route to 1-silacyclopenta-2,4-dienes. *J. Organomet. Chem.* **1981**, *217*, 43−50. (b) Ishikawa, M.; Ohshita, J.; Ito, Y.; Iyoda, J. Silicon-carbon unsaturated compounds. 22. The formation and reactions of a nickelasilacyclobutene. *J. Am. Chem. Soc.* **1986**, *108*, 7417−7419. (c) Ohshita, J.; Isomura, Y.; Ishikawa, M. Silicon-carbon unsaturated compounds. 24. Some reactions of a nickelasilacyclobutene. *Organometallics* **1989**, *8*, 2050−2054. (d) Ohshita, J.; Hasebe,

https://doi.org/10.1021/acs.inorgchem.3c00045
Inorg. Chem. XXXX, XXX, XXX−XXX

H.; Masaoka, Y.; Ishikawa, M. Silicon-Carbon Unsaturated Compounds. 49. Nickel-Catalyzed Reactions of 2-Adamantyl-2-(trimethylsiloxy)-1,1-bis(trimethylsilyl)silene. *Organometallics* **1994**, *13*, 1064−1066.

(25) (a) Tanabe, M.; Osakada, K. Structure of 4-Sila-3-platinacyclobutene and Its Formation via Pt-Promoted γ-Si−H Bond Activation of 3-Sila-1-propenylplatinum Precursor. *J. Am. Chem. Soc.* **2002**, *124*, 4550−4551. (b) Tanabe, M.; Osakada, K. Insertion of Alkynes into the Pt−Si Bond of Silylplatinum Complexes Leading to the Formation of 4-Sila-3-platinacyclobutenes and 5-Sila-2-platina-1,4-cyclohexadienes. *Chem.—Eur. J.* **2004**, *10*, 416−424. (c) Lee, V. Y.; Aoki, S.; Yokoyama, T.; Horiguchi, S.; Sekiguchi, A.; Gornitzka, H.; Guo, J.-D.; Nagase, S. Toward a Silicon Version of Metathesis: From Schrock-Type Titanium Silylidenes to Silatitanacyclobutenes. *J. Am. Chem. Soc.* **2013**, *135*, 2987−2990. (d) Hadlington, T. J.; Kostenko, A.; Driess, M. Cycloaddition Chemistry of a Silylene-Nickel Complex toward Organic pi-Systems: From Reversibility to C-H Activation. *Chem. - Eur. J.* **2020**, *26*, 1958−1962.

(26) The process is equilibrated and the oxidative addition proceeds with release of one equivalent of phosphine that can in turn bind remaining $[(PR_3)_2Pd]$ starting material in the medium. $[(PR_3)_2Pd]$ complex is actually in equilibrium regarding to ligand redistribution and $[Pd(PR_3)_n]$ species as well as free phoshine can be observed.

(27) In the case of $\mathbf{E}^{\mathbf{R}}$, the considerably upfield shifted signal in the ^{29}Si NMR results from the strong contribution of the terminal titanium silylene-alkyne π-complex to the overall structure (see ref 25c).

(28) Pan, Y.; Young, G. B. Syntheses and spectroscopic characteristics of dialkylpalladium(II) complexes; PdR2(cod) as precursors for derivatives with N- or P-donor ligands. *J. Organomet. Chem.* **1999**, *577*, 257−264.

(29) (a) McAtee, J. R.; Martin, S. E.; Ahneman, D. T.; Johnson, K. A.; Watson, D. A. Preparation of allyl and vinyl silanes by the palladium-catalyzed silylation of terminal olefins: a silyl-Heck reaction. *Angew. Chem., Int. Ed.* **2012**, *51*, 3663−3667. (b) Rojas, A. J.; Pentelute, B. L.; Buchwald, S. L. Water-Soluble Palladium Reagents for Cysteine S-Arylation under ASmbient Aqueous Conditions. *Org. Lett.* **2017**, *19*, 4263−4266.

(30) (a) Irie, M. Diarylethenes for Memories and Switches. *Chem. Rev.* **2000**, *100*, 1685−1716. (b) Irie, M.; Fukaminato, T.; Matsuda, K.; Kobatake, S. Photochromism of Diarylethene Molecules and Crystals: Memories, Switches, and Actuators. *Chem. Rev.* **2014**, *114*, 12174−12277.

(31) The existence of the equilibrium was ascertained, in the case of $\mathbf{6\text{-}PPh_3}$, by the presence of cross-peaks in the ^{1}H−^{1}H and ^{31}P−^{31}P NOESY NMR spectra that are indicative of an exchange process.

(32) Bratovanov, S.; Koźmiński, W.; Fässler, J.; Molnar, Z.; Nanz, D.; Bienz, S. Synthesis and Characterization of 1,2-Disubstituted Vinylsilanes and Their Geometric Differentiation with 3J(29Si,1H)-Coupling Constants. Application of a Novel Heteronuclear J-Resolved NMR Experiment. *Organometallics* **1997**, *16*, 3128−3134.

(33) Compound **5** appears as a 0.68:1 rotameric mixture illustrating the prefered positionning of the thienyl groups within the molecule.[30] This well-known feature in DTE-based photochromic molecules was confirmed by low temperature analysis of a pure sample of **5**.

(34) Schager, F.; Bonrath, W.; Pörschke, K.-R.; Kessler, M.; Krüger, C.; Seevogel, K. (R2PC2H4PR2)Pd0−1-Alkyne Complexes. *Organometallics* **1997**, *16*, 4276−4286.

(35) (a) Amatore, C.; Pfluger, F. Mechanism of oxidative addition of palladium(0) with aromatic iodides in toluene, monitored at ultramicroelectrodes. *Organometallics* **1990**, *9*, 2276−2282. (b) Amatore, C.; Jutand, A.; Khalil, F.; M'Barki, M. A.; Mottier, L. Rates and mechanisms of oxidative addition to zerovalent palladium complexes generated in situ from mixtures of Pd0(dba)2 and triphenylphosphine. *Organometallics* **1993**, *12*, 3168−3178.

(36) Although the HOMO orbital is mainly made of a Pd d or-bital, it also partially describes the C1−C2 bond, with the overlapping of two sp hybridized orbitals, as well as the Si−C1 and Si−Pd bonds, via the overlapping of a Si p or-bital with both the C1 sp hybrid on one side and the Pd d orbital on the other side. The HOMO-4 accounts for the Si−C1 and Pd−C2 bonds, involving a first overlapping between a sp hybrid on C1 and a p orbital on Si and a sec-ond overlapping between a sp hybridized orbital on C2 and a d orbital on the Pd metal. The HOMO-7 orbital mainly describes the C1−C2 bond, through the interaction between sp orbitals, whereas the HOMO-10 mainly de-scribed the Si−Pd bond, via the interaction between a p orbital on the Si center and a d orbital on Pd. The HOMO-18 orbital, finally, displays the overlapping of a C2 sp hybridized orbital with both a Pd d orbital on one side and a C1 sp hybridized orbital on the other side, together with an additional slight bonding interaction between the same C1 sp hybridized orbital and a Si p orbital.

(37) For sake of clarity, the LUMO is also depicted in Figure S3-DFT. It consists of an antibonding interaction between the Si and Pd atoms together with a bonding interaction between Pd and phosphorus.

(38) To get more insight into the coordination of the alkyne to **C** ($\mathbf{6\text{-}PPh_3}$), we computed the molecular orbitals of complex **D**. As shown in Figure S5-DFT, the orbital accounting for the bonding with phenylacetylene is the homo-7 one, resulting from the overlapping between the homo orbital of **C** and the lumo orbital of phenylacetylene. Only the Pd metal interacts with phenylacetylene, a Pd d orbital overlapping the π* orbital of the alkyne C−C bond.

(39) (a) Zhao, Y.; Truhlar, D. G. Density Functionals with Broad Applicability in Chemistry. *Acc. Chem. Res.* **2008**, *41*, 157−167. (b) Schultz, N. E.; Zhao, Y.; Truhlar, D. G. Benchmarking approximate density functional theory for s/d excitation energies in 3d transition metal cations. *J. Comput. Chem.* **2008**, *29*, 185−189.

https://doi.org/10.1021/acs.inorgchem.3c00045
Inorg. Chem. XXXX, XXX, XXX−XXX